PHYSICAL REVIEW D **89,** 054037 (2014)

Exotic open-flavor $bc\bar{q}\,\bar{q}$, $bc\bar{s}\,\bar{s}$ and $qc\bar{q}\,\bar{b}$, $sc\bar{s}\,\bar{b}$ tetraquark states

Wei Chen,[1,*] T. G. Steele,[1,†] and Shi-Lin Zhu[2,‡]

[1]*Department of Physics and Engineering Physics, University of Saskatchewan, Saskatoon, Saskatchewan S7N 5E2, Canada*

[2]*Department of Physics and State Key Laboratory of Nuclear Physics and Technology, Peking University, Beijing 100871, China, and Collaborative Innovation Center of Quantum Matter, Beijing 100871, China*

(Received 7 November 2013; published 28 March 2014)

We study the exotic $bc\bar{q}\,\bar{q}$, $bc\bar{s}\,\bar{s}$ and $qc\bar{q}\,\bar{b}$, $sc\bar{s}\,\bar{b}$ systems by constructing the corresponding tetraquark currents with $J^P = 0^+$ and 1^+. After investigating the two-point correlation functions and the spectral densities, we perform QCD sum rule analysis and extract the masses of these open-flavor tetraquark states. Our results indicate that the masses of both the scalar and axial vector tetraquark states are about 7.1–7.2 GeV for the $bc\bar{q}\,\bar{q}$ system and 7.2–7.3 GeV for the $bc\bar{s}\,\bar{s}$ system. For the $qc\bar{q}\,\bar{b}$ tetraquark states with $J^P = 0^+$ and 1^+, their masses are extracted to be around 7.1 GeV. The masses for the scalar and axial vector $sc\bar{s}\,\bar{b}$ states are 7.1 and 6.9–7.1 GeV, respectively. The tetraquark states $qc\bar{q}\,\bar{b}$ and $sc\bar{s}\,\bar{b}$ lie below the thresholds of $D^{(*)}B^{(*)}$ and $D_s^{(*)}B_s^{(*)}$ respectively, but they can decay into B_c plus a light meson. However, the tetraquark states $bc\bar{q}\,\bar{q}$ and $bc\bar{s}\,\bar{s}$ lie below the $D^{(*)}\bar{B}^{(*)}$ and $D_s^{(*)}\bar{B}_s^{(*)}$ thresholds, suggesting dominantly weak decay mechanisms.

DOI: 10.1103/PhysRevD.89.054037 PACS numbers: 12.39.Mk, 12.38.Lg, 14.40.Lb, 14.40.Nd

I. INTRODUCTION

In the conventional quark model a meson is composed of a pair of quark and antiquark ($q\bar{q}$) and a baryon is composed of three quarks (qqq) [1,2]. However, quantum chromodynamics (QCD) allows more complicated hadron configurations. Hadrons with structures different from $q\bar{q}/qqq$ are sometimes called "exotic" states. Although none of the exotic states is now unambiguously identified, more and more unexpected charmoniumlike and bottomoniumlike states have been observed in the past several years. These resonances are considered as important candidates of exotic hadrons, such as hadronic molecules, tetraquark states, hybrids, etc.

The possible existence of the tetraquarks ($qq\bar{q}\,\bar{q}$) composed of a diquark and an antidiquark was suggested by Jaffe in 1977 [3,4]. The frequently discussed candidates of tetraquark states are the light scalars [3–7]. In the heavy quark sector, $qQ\bar{q}\,\bar{Q}$-type hidden-flavor tetraquarks have been extensively studied to explain the underlying structures of the recently observed XYZ states in the relativistic quark model [8,9], QCD sum rules [10–14] and via bound diquark clusters [15–18]. The existence and stability of doubly charmed/bottomed $QQ\bar{q}\,\bar{q}$ tetraquark states have been also studied in the MIT bag model [19], chiral quark model [20,21], constituent quark model [22–26], relativistic quark model [27], chiral perturbation theory [28], QCD sum rules [29–32] and some other methods [33–40].

Recently, there have been efforts to understand the open-flavor (i.e., exotic) tetraquark states $bc\bar{q}\,\bar{q}$ [25,26,41] and molecular states $\bar{q}c\bar{b}q$ [42–44]. The authors of Ref. [41] noticed that the tetraquark states $bc\bar{q}\,\bar{q}$ lie below the thresholds of B^-D^+ and $\bar{B}^0D^0$ by solving the Bethe-Salpeter equations. In Refs. [43,44], the authors indicated that there may exist loosely bound B_c-like molecular states. In this paper, we will study the open-flavor $bc\bar{q}\,\bar{q}$, $bc\bar{s}\,\bar{s}$ and $qc\bar{q}\,\bar{b}$, $sc\bar{s}\,\bar{b}$ tetraquark states in QCD sum rules. We construct the corresponding tetraquark currents with $J^P = 0^+, 1^+$ by using S-wave diquark fields. With these interpolating operators, we calculate the two-point correlation functions and extract the masses of these possible tetraquark states.

This paper is organized as follows. In Sec. II, we construct all the scalar and axial vector $bc\bar{q}\,\bar{q}$, $bc\bar{s}\,\bar{s}$ and $qc\bar{q}\,\bar{b}$, $sc\bar{s}\,\bar{b}$ types of tetraquark currents with S-wave diquark fields and the corresponding antidiquark fields. In Sec. III, we calculate the two-point correlation functions and the spectral densities using these interpolating tetraquark currents. The expressions for the spectral densities are listed in the Appendix. We perform QCD sum rule analysis for these tetraquark systems and extract their masses in Sec. IV. We also construct mixed interpolating currents to study mixing effects. In the final section, we summarize our results and discuss the possible decay properties of these tetraquark states.

II. TETRAQUARK INTERPOLATING CURRENTS

In this section, we construct the $bc\bar{q}\,\bar{q}$ and $qc\bar{q}\,\bar{b}$ types of tetraquark interpolating currents using diquark and antidiquark fields. In general, one can use the diquark

*wec053@mail.usask.ca
†tom.steele@usask.ca
‡zhusl@pku.edu.cn

fields $q_a^TCq_b$, $q_a^TC\gamma_5q_b$, $q_a^TC\gamma_\mu q_b$, $q_a^TC\gamma_\mu\gamma_5q_b$, $q_a^TC\sigma_{\mu\nu}q_b$, $q_a^TC\sigma_{\mu\nu}\gamma_5q_b$ and the corresponding antidiquark fields to compose all possible combinations of $bc\bar{q}\,\bar{q}$ and $qc\bar{q}\,\bar{b}$ tetraquark operators, as done in Ref. [30] for the doubly charmed/bottomed tetraquark states and Refs. [12,13] for the charmoniumlike and bottomoniumlike tetraquark states. In Ref. [30], the tetraquark currents which contain P-wave diquark or antidiquark operators can result in higher hadron masses than those containing only S-wave operators. They correspond to the orbitally excited states while the latter operators correspond to the ground hadron states. In order to study the lowest lying tetraquark states, we use only the S-wave diquark fields $q_a^TC\gamma_5q_b$, $q_a^TC\gamma_\mu q_b$ and the corresponding antidiquark fields to compose the tetraquark currents with quantum numbers $J^P=0^+,\ 1^+$. The P-wave diquark fields will not be considered in this paper.

For the $bc\bar{q}\,\bar{q}$ system, the tetraquark interpolating currents with $J^P=0^+$ are

$$
\begin{aligned}
J_1 &= b_a^TC\gamma_5c_b(\bar{q}_a\gamma_5C\bar{q}_b^T+\bar{q}_b\gamma_5C\bar{q}_a^T),\\
J_2 &= b_a^TC\gamma_\mu c_b(\bar{q}_a\gamma^\mu C\bar{q}_b^T+\bar{q}_b\gamma^\mu C\bar{q}_a^T),\\
J_3 &= b_a^TC\gamma_5c_b(\bar{q}_a\gamma_5C\bar{q}_b^T-\bar{q}_b\gamma_5C\bar{q}_a^T),\\
J_4 &= b_a^TC\gamma_\mu c_b(\bar{q}_a\gamma^\mu C\bar{q}_b^T-\bar{q}_b\gamma^\mu C\bar{q}_a^T),
\end{aligned}\tag{1}
$$

in which "+" denotes the symmetric color structure $[\mathbf{6_c}]_{bc}\otimes[\bar{\mathbf{6}}_\mathbf{c}]_{\bar{q}\,\bar{q}}$ and "−" denotes the antisymmetric color structure $[\bar{\mathbf{3}}_\mathbf{c}]_{bc}\otimes[\mathbf{3_c}]_{\bar{q}\,\bar{q}}$. The tetraquark interpolating currents with $J^P=1^+$ are

$$
\begin{aligned}
J_{1\mu} &= b_a^TC\gamma_5c_b(\bar{q}_a\gamma_\mu C\bar{q}_b^T+\bar{q}_b\gamma_\mu C\bar{q}_a^T),\\
J_{2\mu} &= b_a^TC\gamma_\mu c_b(\bar{q}_a\gamma_5 C\bar{q}_b^T+\bar{q}_b\gamma_5 C\bar{q}_a^T),\\
J_{3\mu} &= b_a^TC\gamma_5c_b(\bar{q}_a\gamma_\mu C\bar{q}_b^T-\bar{q}_b\gamma_\mu C\bar{q}_a^T),\\
J_{4\mu} &= b_a^TC\gamma_\mu c_b(\bar{q}_a\gamma_5 C\bar{q}_b^T-\bar{q}_b\gamma_5 C\bar{q}_a^T),
\end{aligned}\tag{2}
$$

where + again denotes the symmetric color structure $[\mathbf{6_c}]_{bc}\otimes[\bar{\mathbf{6}}_\mathbf{c}]_{\bar{q}\,\bar{q}}$ and − denotes the antisymmetric color structure $[\bar{\mathbf{3}}_\mathbf{c}]_{bc}\otimes[\mathbf{3_c}]_{\bar{q}\,\bar{q}}$.

Similarly, for the $cq\bar{b}\,\bar{q}$ system, the tetraquark interpolating currents with $J^P=0^+$ are

$$
\begin{aligned}
J_1 &= q_a^TC\gamma_5c_b(\bar{q}_a\gamma_5C\bar{b}_b^T+\bar{q}_b\gamma_5C\bar{b}_a^T),\\
J_2 &= q_a^TC\gamma_\mu c_b(\bar{q}_a\gamma^\mu C\bar{b}_b^T+\bar{q}_b\gamma^\mu C\bar{b}_a^T),\\
J_3 &= q_a^TC\gamma_5c_b(\bar{q}_a\gamma_5C\bar{b}_b^T-\bar{q}_b\gamma_5C\bar{b}_a^T),\\
J_4 &= q_a^TC\gamma_\mu c_b(\bar{q}_a\gamma^\mu C\bar{b}_b^T-\bar{q}_b\gamma^\mu C\bar{b}_a^T),
\end{aligned}\tag{3}
$$

in which + denotes the symmetric color structure $[\mathbf{6_c}]_{qc}\otimes[\bar{\mathbf{6}}_\mathbf{c}]_{\bar{q}\,\bar{b}}$ and − denotes the antisymmetric color structure $[\bar{\mathbf{3}}_\mathbf{c}]_{qc}\otimes[\mathbf{3_c}]_{\bar{q}\,\bar{b}}$. The tetraquark interpolating currents with $J^P=1^+$ are

$$
\begin{aligned}
J_{1\mu} &= q_a^TC\gamma_5c_b(\bar{q}_a\gamma_\mu C\bar{b}_b^T+\bar{q}_b\gamma_\mu C\bar{b}_a^T),\\
J_{2\mu} &= q_a^TC\gamma_\mu c_b(\bar{q}_a\gamma_5 C\bar{b}_b^T+\bar{q}_b\gamma_5 C\bar{b}_a^T),\\
J_{3\mu} &= q_a^TC\gamma_5c_b(\bar{q}_a\gamma_\mu C\bar{b}_b^T-\bar{q}_b\gamma_\mu C\bar{b}_a^T),\\
J_{4\mu} &= q_a^TC\gamma_\mu c_b(\bar{q}_a\gamma_5 C\bar{b}_b^T-\bar{q}_b\gamma_5 C\bar{b}_a^T),
\end{aligned}\tag{4}
$$

where + again denotes the symmetric color structure $[\mathbf{6_c}]_{qc}\otimes[\bar{\mathbf{6}}_\mathbf{c}]_{\bar{q}\,\bar{b}}$ and − denotes the antisymmetric color structure $[\bar{\mathbf{3}}_\mathbf{c}]_{qc}\otimes[\mathbf{3_c}]_{\bar{q}\,\bar{b}}$.

Replacing the light quark q by the strange quark s in Eqs. (3) and (4), we can also obtain the corresponding $cs\bar{b}\,\bar{s}$ tetraquark currents with the same quantum numbers. However, the $bc\bar{s}\,\bar{s}$ system is different. In this system, the flavor structure of $\bar{s}\,\bar{s}$ pair is symmetric and thus its color structure is fixed at the same time. The color structures for the diquark fields $s_a^TC\gamma_5s_b$ and $s_a^TC\gamma_\mu s_b$ are symmetric $\mathbf{6_c}$ and antisymmetric $\bar{\mathbf{3}}_\mathbf{c}$, respectively. As a result, only J_1, J_4 in Eq. (1) and $J_{2\mu}$, $J_{3\mu}$ in Eq. (2) survive in the $bc\bar{s}\,\bar{s}$ system and all the other currents vanish.

III. TWO-POINT CORRELATION FUNCTION AND SPECTRAL DENSITY

In the framework of QCD sum rules [45–47], we consider the two-point correlation functions

$$
\Pi(p^2)=i\int d^4xe^{ip\cdot x}\langle 0|T[J(x)J^\dagger(0)]|0\rangle,\tag{5}
$$

$$
\Pi_{\mu\nu}(p^2)=i\int d^4xe^{ip\cdot x}\langle 0|T[J_\mu(x)J_\nu^\dagger(0)]|0\rangle,\tag{6}
$$

where $J(x)$ and $J_\mu(x)$ are the scalar and axial vector currents shown in Eqs. (1)–(4). Since the axial vector currents $J_\mu(x)$ are not conserved, the two-point correlation function $\Pi_{\mu\nu}(p^2)$ has the following structure:

$$
\Pi_{\mu\nu}(p^2)=\left(\frac{p_\mu p_\nu}{p^2}-g_{\mu\nu}\right)\Pi_1(p^2)+\frac{p_\mu p_\nu}{p^2}\Pi_0(p^2),\tag{7}
$$

where $\Pi_1(p^2)$ and $\Pi_0(p^2)$ are the invariant functions related to the spin-1 and spin-0 intermediate states, respectively. In this paper, we focus on $\Pi_1(p^2)$ to study the axial vector channels.

In QCD sum rules, the correlation functions in Eqs. (5) and (6) can be obtained at both the hadron level and quark-gluon level. At the hadron level, we can describe the correlation function via the dispersion relation

$$\Pi(p^2) = (p^2)^N \int_{(m_c+m_b)^2}^{\infty} \frac{\rho(s)}{s^N(s-p^2-i\epsilon)} ds + \sum_{n=0}^{N-1} b_n (p^2)^n, \tag{8}$$

in which b_n are the N unknown subtraction constants which can be removed by taking the Borel transform. To obtain the spectral function $\rho(s)$, we write the imaginary part of $\Pi(p^2)$ as a sum over δ functions by inserting intermediate hadronic states $|n\rangle$ with the same quantum numbers as the interpolating current $J(x)$,

$$\rho(s) \equiv \frac{1}{\pi}\mathrm{Im}\Pi(s) = \sum_n \delta(s-m_n^2)\langle 0|J|n\rangle\langle n|J^\dagger|0\rangle = f_X^2\delta(s-m_X^2) + \text{continuum}, \tag{9}$$

where we adopt the pole plus continuum parametrization of the hadronic spectral density and m_X is the mass of the lowest lying resonance $|X\rangle$. The scalar and axial vector interpolating currents $J(x)$ and $J_\mu(x)$ can couple to the corresponding hadronic states with the coupling parameters f_X,

$$\langle 0|J|X\rangle = f_X, \tag{10}$$

$$\langle 0|J_\mu|X\rangle = f_X\epsilon_\mu, \tag{11}$$

where ϵ_μ is the polarization vector ($\epsilon \cdot p = 0$).

The correlation function can also be evaluated at the quark-gluon level via the operator product expansion (OPE) method. We calculate the Wilson coefficients up to dimension eight at leading order in α_s. Utilizing the same technique as in Refs. [12–14,30,48], we adopt the coordinate expression for the light quark propagator and the momentum space expression for the heavy quark propagator,

$$\begin{aligned} iS_q^{ab}(x) = {} & \frac{i\delta^{ab}}{2\pi^2x^4}\hat{x} + \frac{i}{32\pi^2}\frac{\lambda_{ab}^n}{2}g_sG_{\mu\nu}^n\frac{1}{x^2}(\sigma^{\mu\nu}\hat{x}+\hat{x}\sigma^{\mu\nu}) \\ & - \frac{\delta^{ab}}{12}\langle\bar{q}q\rangle + \frac{\delta^{ab}x^2}{192}\langle\bar{q}g_s\sigma\cdot Gq\rangle - \frac{m_q\delta^{ab}}{4\pi^2x^2} \\ & + \frac{i\delta^{ab}m_q\langle\bar{q}q\rangle}{48}\hat{x} - \frac{im_q\langle\bar{q}g_s\sigma\cdot Gq\rangle\delta^{ab}x^2\hat{x}}{1152}, \end{aligned} \tag{12}$$

$$\begin{aligned} iS_Q^{ab}(p) = {} & \frac{i\delta^{ab}}{\hat{p}-m_Q} + \frac{i}{4}g_s\frac{\lambda_{ab}^n}{2}G_{\mu\nu}^n \\ & \times\frac{\sigma^{\mu\nu}(\hat{p}+m_Q)+(\hat{p}+m_Q)\sigma^{\mu\nu}}{(p^2-m_Q^2)^2} \\ & + \frac{i\delta^{ab}}{12}\langle g_s^2GG\rangle m_Q\frac{p^2+m_Q\hat{p}}{(p^2-m_Q^2)^4}, \end{aligned} \tag{13}$$

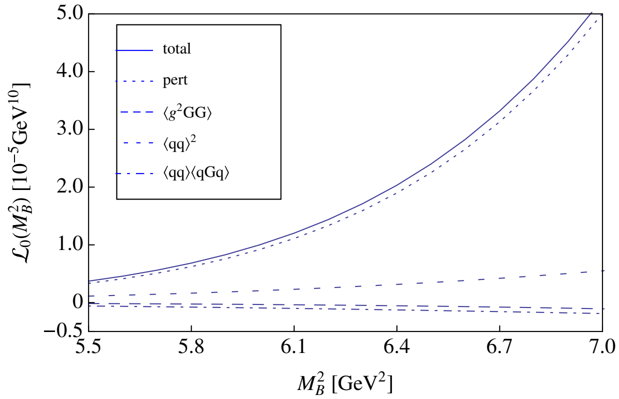

FIG. 1 (color online). OPE convergence for the current J_4 in the $J^P = 0^+ bc\bar{q}\,\bar{q}$ system.

in which q represents u, d, or s quark and Q represents c or b quark. The superscripts a, b are color indices and $\hat{x} = \gamma_\mu x^\mu$, $\hat{p} = \gamma_\mu p^\mu$. We keep the terms proportional to m_q to study the $sc\bar{s}\,\bar{b}$ and $bc\bar{s}\,\bar{s}$ systems. In particular, the m_s corrections are only important for the chiral-violating condensates; the m_q corrections to the gluon condensate that would arise from an m_q term in (12) are numerically small and are thus ignored (see Fig. 1 below).

By equating the correlation functions at both the hadron level and quark-gluon level, we can establish the sum rules for the hadron parameters via quark-hadron duality. Using the spectral function defined in Eq. (9), the Borel transform is performed on the correlation function $\Pi(p^2)$ obtained at both levels to remove the unknown constants in Eq. (8), improve the convergence of the OPE series, and suppress the continuum contributions

$$\mathcal{L}_k(s_0, M_B^2) = f_X^2 m_X^{2k} e^{-m_X^2/M_B^2} = \int_{(m_c+m_b)^2}^{s_0} ds e^{-s/M_B^2}\rho(s)s^k, \tag{14}$$

where s_0 is the continuum threshold parameter and M_B is the Borel mass introduced by the Borel transform. These two parameters are very important in QCD sum rule analysis and we will discuss them carefully in the next section. Then the mass of the lowest lying hadron state can be extracted as

$$m_X(s_0, M_B^2) = \sqrt{\frac{\mathcal{L}_1(s_0, M_B^2)}{\mathcal{L}_0(s_0, M_B^2)}}, \tag{15}$$

which is a function of the continuum threshold s_0 and Borel mass M_B. At the leading order in α_s, the spectral densities for all interpolating currents in Eqs. (1)–(4) are evaluated and listed in the Appendix up to dimension eight condensates. For the nonperturbative contributions, the quark condensate $\langle\bar{q}q\rangle$, gluon condensate $\langle GG\rangle$, quark-gluon condensate mixed $\langle\bar{q}g_s\sigma\cdot Gq\rangle$, four quark condensate and dimension eight condensate contribute to the correlation functions and spectral densities. Using the factorization hypothesis, the dimension six and eight condensates are reduced to $\langle\bar{q}q\rangle^2$ and $\langle\bar{q}q\rangle\langle\bar{q}g_s\sigma\cdot Gq\rangle$ respectively. The evaluation of the higher dimension condensate contributions is technically difficult and the violation of the factorization hypothesis becomes important [49]. In this paper, we calculate the correlation functions up to dimension eight.

IV. QCD SUM RULE ANALYSIS

To perform the QCD sum rule analysis, we adopt the following values of the quark masses and various condensates [2,46,50–52] in the chiral limit ($m_u = m_d = 0$):

$$\begin{aligned} m_s(2\text{ GeV}) &= (101^{+29}_{-21})\text{ MeV},\\ m_c(\mu=m_c) &= \bar{m}_c = (1.28\pm 0.02)\text{ GeV},\\ m_b(\mu=m_b) &= \bar{m}_b = (4.17\pm 0.02)\text{ GeV},\\ \langle\bar{q}q\rangle &= -(0.23\pm 0.03)^3\text{ GeV}^3,\\ \langle\bar{q}g_s\sigma\cdot Gq\rangle &= -M_0^2\langle\bar{q}q\rangle,\\ M_0^2 &= (0.8\pm 0.2)\text{ GeV}^2,\\ \langle\bar{s}s\rangle/\langle\bar{q}q\rangle &= 0.8\pm 0.1,\\ \langle g_s^2GG\rangle &= (0.48\pm 0.14)\text{ GeV}^4, \end{aligned} \tag{16}$$

in which the definition of the coupling constant g_s has a minus sign difference compared to that in Ref. [46]. The charm and bottom quark masses are the running masses in the $\overline{\text{MS}}$ scheme. Furthermore, we take into account the scale dependence of these $\overline{\text{MS}}$ masses at leading order:

$$m_c(\mu) = \bar{m}_c\left(\frac{\alpha_s(\mu)}{\alpha_s(\bar{m}_c)}\right)^{12/25}, \tag{17}$$

$$m_b(\mu) = \bar{m}_b\left(\frac{\alpha_s(\mu)}{\alpha_s(\bar{m}_b)}\right)^{12/23}, \tag{18}$$

where

$$\alpha_s(\mu) = \frac{\alpha_s(M_\tau)}{1+\frac{25\alpha_s(M_\tau)}{12\pi}\log(\frac{\mu^2}{M_\tau^2})}, \qquad \alpha_s(M_\tau) = 0.33 \tag{19}$$

is determined by evolution from the τ mass using Particle Data Group values [2]. For the $bc\bar{q}\,\bar{q}$ and $qc\bar{q}\,\bar{b}$ tetraquark systems, we use the renormalization scale $\mu = \frac{\bar{m}_c+\bar{m}_b}{2} = 2.73$ GeV in our sum rule analysis [53].

After performing the Borel transform, there are two important parameters in the correlation function: the continuum threshold s_0 and the Borel mass M_B. The stability of QCD sum rules requires a suitable working region of these two parameters. In our analysis, we choose the value of s_0 to minimize the variation of the extracted mass m_X with the Borel mass M_B^2. Using this value of s_0, we can obtain a suitable Borel window by studying the convergence of the OPE series and pole contribution. The requirement of the OPE convergence determines a lower bound on M_B^2 while the constraint of the pole contribution leads to its upper bound.

The pole contribution (PC) is defined as

$$\text{PC}(s_0, M_B^2) = \frac{\mathcal{L}_0(s_0, M_B^2)}{\mathcal{L}_0(\infty, M_B^2)}, \tag{20}$$

which is a function of the continuum threshold s_0 and the Borel mass M_B. This definition comes from the sum rules established in Eq. (14) and indicates the contribution of the lowest lying resonance to the correlation function.

A. $bc\bar{q}\,\bar{q}$ and $bc\bar{s}\,\bar{s}$ tetraquark systems

We begin with the sum rule analysis of the $bc\bar{q}\,\bar{q}$ and $bc\bar{s}\,\bar{s}$ tetraquark systems in this subsection. For all currents in the $bc\bar{q}\,\bar{q}$ systems, the quark condensate $\langle\bar{q}q\rangle$ and quark gluon mixed condensate $\langle\bar{q}g_s\sigma\cdot Gq\rangle$ terms in the correlation functions are proportional to the light quark mass m_q. Both of them vanish in chiral limit $m_q = 0$ and represent a numerically small contribution to the correlation functions because of this chiral suppression. For these systems, the four quark condensate $\langle\bar{q}q\rangle^2$ is the dominant power correction to the correlation function. We show the OPE convergence of the scalar $bc\bar{q}\,\bar{q}$ channel using the interpolating current J_4 in Fig. 1. It indicates that the dimension eight condensate $\langle\bar{q}q\rangle\langle\bar{q}g_s\sigma\cdot Gq\rangle$ is the next in importance followed by the gluon condensate $\langle GG\rangle$. To ensure the convergence of the OPE series, we require that the four quark condensate contribution be less than one-fifth of the perturbative term, which results in a lower bound on the Borel mass M_B. In Fig. 1, the OPE convergence is very good in the region $M_B^2 \geq 6.1$ GeV^2. This value is the lower bound on M_B^2 for J_4 scalar channel of $bc\bar{q}\,\bar{q}$ system.

On the other hand, an upper bound on M_B^2 is obtained by studying the pole contribution defined in Eq. (20), which is also the function of the continuum threshold s_0. To study the variation of PC with M_B, one should determine the value of s_0 at first. An optimized choice of s_0 is the value minimizing the variation of the extracted hadron mass m_X with the Borel parameter M_B^2. We study this in the left portion of Fig. 2 for the scalar $bc\bar{q}\,\bar{q}$ channel with the current J_4. Varying the value of M_B^2 from its lower bound $M^2_{\text{min}} = 6.1$ GeV^2, these mass curves with different value of M_B^2 intersect at $s_0 = 60$ GeV^2, which is the most suitable value under the above constraint. Utilizing this value of s_0, we require that PC be larger than 30% to determine the upper bound on the Borel mass M_B^2. For the current J_4 in the scalar $bc\bar{q}\,\bar{q}$ channel, we obtain the upper bound $M^2_{\text{max}} = 6.4$ GeV^2.

For the $J^P = 0^+ bc\bar{q}\,\bar{q}$ systems, all currents J_1, J_2, J_3 and J_4 have suitable working range of the Borel parameter with

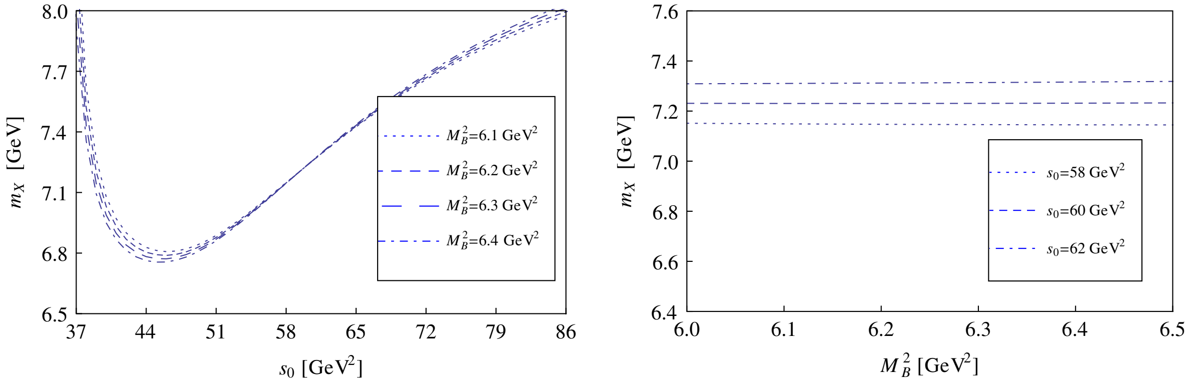

FIG. 2 (color online). Variation of m_X with s_0 and M_B^2 corresponding to the current J_4 for the $0^+bc\bar{q}\,\bar{q}$ system.

the above criteria. Within these Borel windows, the mass sum rules are very stable. In Fig. 2, we show the variation of m_X with the threshold value s_0 and Borel parameter M_B^2 for the current J_4. We obtain the Borel window $6.1\ \mathrm{GeV}^2 \le M_B^2 \le 6.4\ \mathrm{GeV}^2$ with the continuum threshold value $s_0 = 60\ \mathrm{GeV}^2$. In this region, we show the stable mass sum rule in the right portion of Fig. 2 and extract the hadron mass

$$m_X = 7.23 \pm 0.08 \pm 0.05 \pm 0.06\ \mathrm{GeV}, \qquad (21)$$

in which the errors come respectively from the continuum threshold s_0, the heavy quark masses m_c, m_b and the quark condensates $\langle\bar{q}q\rangle, \langle\bar{q}g_s\sigma\cdot Gq\rangle$. The errors from the Borel mass M_B and the gluon condensate $\langle g_s^2GG\rangle$ are negligible since the mass sum rules are very stable in the Borel window (see Figs. 2 and 3) while, as mentioned above, the gluon condensate contribution to the correlation function is very small.

After performing the QCD sum rule analyses for all the interpolating currents, we collect the Borel window, the threshold value, the extracted mass and the pole contribution for the $J^P = 0^+bc\bar{q}\,\bar{q}$ systems in Table I. The results for the $J^P = 1^+bc\bar{q}\,\bar{q}$ systems are listed in Table II. As mentioned above, the errors of mass predictions come from the uncertainties in s_0, the heavy quark masses m_c, m_b and QCD condensates $\langle\bar{q}q\rangle, \langle\bar{q}g_s\sigma\cdot Gq\rangle$ respectively.

The above analyses can easily be extended to the $bc\bar{s}\,\bar{s}$ systems by replacing the corresponding parameters such as the light quark mass and various condensates. We expand the spectral densities to first order in m_s because m_s is much larger than m_q and thus cannot be omitted. These terms are very important to the OPE convergence and the mass sum rule stability for the $bc\bar{s}\,\bar{s}$ systems. As mentioned in Sec. II, only J_1, J_4 with $J^P = 0^+$ in Eq. (1) and $J_{2\mu}$, $J_{3\mu}$ with $J^P = 1^+$ in Eq. (2) survive in the $bc\bar{s}\,\bar{s}$ system. For the currents J_4 with $J^P = 0^+$, we show the variation of the extracted mass m_X with the threshold value s_0 and Borel parameter M_B^2 in Fig. 3. We obtain the threshold value $s_0 = 60\ \mathrm{GeV}^2$ and the Borel window $5.6\ \mathrm{GeV}^2 \le M_B^2 \le 6.5\ \mathrm{GeV}^2$. Compared to the $bc\bar{q}\,\bar{q}$ system, the Borel window of the $bc\bar{s}\,\bar{s}$ system becomes broader because the pole contribution of the $bc\bar{s}\,\bar{s}$ channel is larger than that of the $bc\bar{q}\,\bar{q}$ channel and the OPE convergence becomes better. Finally, we extract the hadron mass around $m_X = 7.26 \pm 0.08 \pm 0.06 \pm 0.10$ GeV. After performing the numerical analyses for all currents, we list the numerical results of the $0^+bc\bar{s}\,\bar{s}$ system in Table I and the $1^+bc\bar{s}\,\bar{s}$ system in Table II. For the same current and QCD input parameters, the extracted mass of the $bc\bar{s}\,\bar{s}$ state is about 0.1 GeV higher than that of the $bc\bar{q}\,\bar{q}$ state.

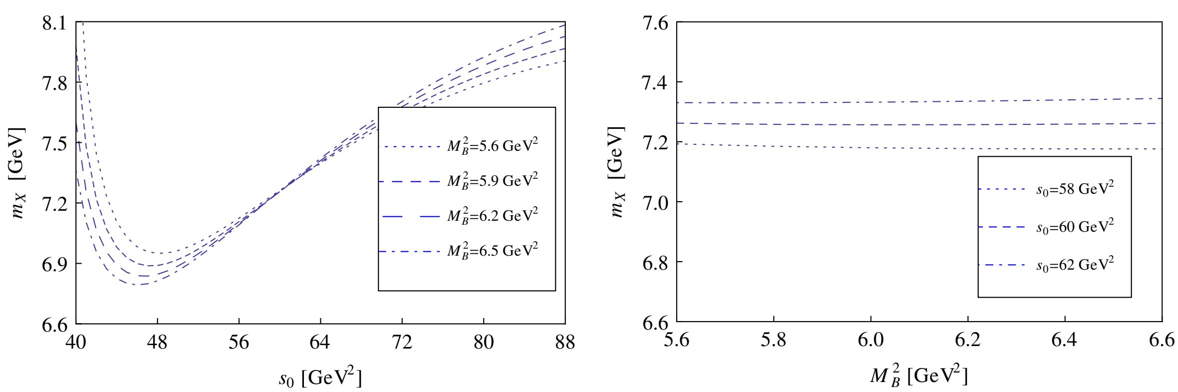

FIG. 3 (color online). Variation of m_X with s_0 and M_B^2 corresponding to the current J_4 for the $0^+bc\bar{s}\,\bar{s}$ system.

TABLE I. The threshold value, Borel window, mass and pole contribution for the $J^P = 0^+ bc\bar{q}\,\bar{q}$ and $bc\bar{s}\,\bar{s}$ systems.

System	Current	$s_0(\mathrm{GeV}^2)$	$[M^2_{\min}, M^2_{\max}]\,(\mathrm{GeV}^2)$	$m_X\,(\mathrm{GeV})$	PC (%)
$bc\bar{q}\,\bar{q}$	J_1	60 ± 2	5.4–6.2	$7.27 \pm 0.08 \pm 0.06 \pm 0.05$	35.5
	J_2	59 ± 2	6.1–6.4	$7.16 \pm 0.09 \pm 0.06 \pm 0.01$	32.9
	J_3	58 ± 2	5.4–6.0	$7.14 \pm 0.08 \pm 0.05 \pm 0.03$	33.9
	J_4	60 ± 2	6.1–6.4	$7.23 \pm 0.08 \pm 0.05 \pm 0.06$	33.5
$bc\bar{s}\,\bar{s}$	J_1	61 ± 2	4.9–6.4	$7.35 \pm 0.08 \pm 0.06 \pm 0.03$	39.1
	J_4	60 ± 2	5.6–6.5	$7.26 \pm 0.08 \pm 0.06 \pm 0.10$	36.7

TABLE II. The threshold value, Borel window, mass and pole contribution for $J^P = 1^+ bc\bar{q}\,\bar{q}$ and $bc\bar{s}\,\bar{s}$ systems.

System	Current	$s_0\,(\mathrm{GeV}^2)$	$[M^2_{\min}, M^2_{\max}]\,(\mathrm{GeV}^2)$	$m_X\,(\mathrm{GeV})$	PC (%)
$bc\bar{q}\,\bar{q}$	$J_{1\mu}$	59 ± 2	5.5–6.1	$7.21 \pm 0.08 \pm 0.05 \pm 0.03$	34.7
	$J_{2\mu}$	60 ± 2	5.3–6.2	$7.27 \pm 0.09 \pm 0.06 \pm 0.05$	37.5
	$J_{3\mu}$	60 ± 2	5.4–6.3	$7.26 \pm 0.08 \pm 0.06 \pm 0.05$	36.8
	$J_{4\mu}$	58 ± 2	5.3–6.0	$7.13 \pm 0.08 \pm 0.06 \pm 0.03$	35.7
$bc\bar{s}\,\bar{s}$	$J_{2\mu}$	61 ± 2	4.9–6.4	$7.35 \pm 0.07 \pm 0.11 \pm 0.04$	41.2
	$J_{3\mu}$	61 ± 2	4.9–6.4	$7.34 \pm 0.07 \pm 0.07 \pm 0.08$	42.1

B. $qc\bar{q}\,\bar{b}$ and $sc\bar{s}\,\bar{b}$ tetraquark systems

In this subsection, we study $qc\bar{q}\,\bar{b}$ and $sc\bar{s}\,\bar{b}$ tetraquark systems with $J^P = 0^+$, 1^+. These configurations are very different from the $bc\bar{q}\,\bar{q}$ and $bc\bar{s}\,\bar{s}$ tetraquark systems. In the correlation functions and the spectral densities, the quark condensate $\langle\bar{q}q\rangle$ and the quark gluon mixed condensate $\langle\bar{q}g_s\sigma\cdot Gq\rangle$ contain terms proportional to the heavy quark masses and they cannot be ignored. They give the most important nonperturbative contributions to the correlation functions. In particular, the quark condensate $\langle\bar{q}q\rangle$ term is now the dominant power correction to the correlation function.

To ensure OPE convergence, we require that the perturbative term be larger than 3 times of the quark condensate to obtain a lower bound on the Borel parameter. Requiring PC be larger than 10% leads to an upper bound on M_B^2. After studying the pole contribution, we find that the PC in all channels for the $qc\bar{q}\,\bar{b}$ and $sc\bar{s}\,\bar{b}$ tetraquark systems are much smaller than those for the $bc\bar{q}\,\bar{q}$ and $bc\bar{s}\,\bar{s}$ tetraquark systems. This means that the Borel windows in the $qc\bar{q}\,\bar{b}$ and $sc\bar{s}\,\bar{b}$ systems will be much narrower than those in the $bc\bar{q}\,\bar{q}$ and $bc\bar{s}\,\bar{s}$ systems.

For the $J^P = 0^+ qc\bar{q}\,\bar{b}$ system, only the current J_1 gives a significant (although narrow) Borel window under the above criteria. The pole contributions of the currents J_2, J_3 and J_4 are too small to give a suitable working region of the Borel mass. In Fig. 4, we show the Borel curves of the extracted mass with the threshold value s_0 and the Borel parameter M_B^2 using the interpolating current J_1. For $s_0 = 55\ \mathrm{GeV}^2$, we obtain a very narrow Borel window $7.8\ \mathrm{GeV}^2 \le M_B^2 \le 8.0\ \mathrm{GeV}^2$. In this region, the mass sum rule is very stable and the hadron mass is finally extracted as $m_X = 7.11$ GeV.

However, the $sc\bar{s}\,\bar{b}$ systems are much better. The interpolating currents J_1, J_2 and J_4 can result in stable mass sum rules and allow reliable extraction of hadron masses. In Fig. 5, we show the Borel curves for the current J_1 in the $sc\bar{s}\,\bar{b}$ system. For $s_0 = 56\ \mathrm{GeV}^2$, the Borel

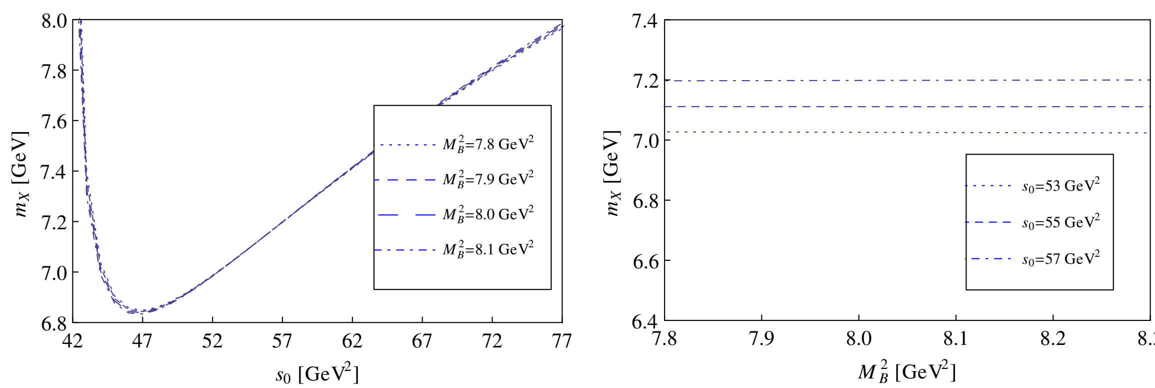

FIG. 4 (color online). Variation of m_X with s_0 and M_B^2 corresponding to the current J_1 for the $0^+ qc\bar{q}\,\bar{b}$ system.

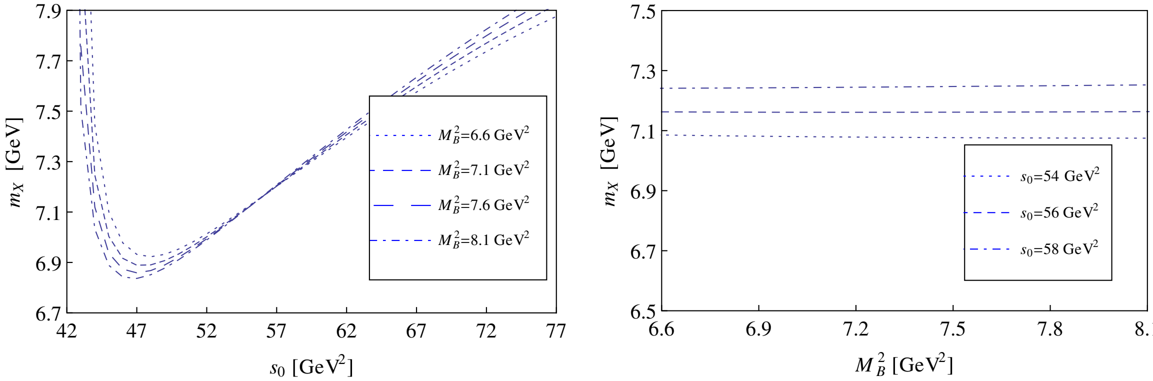

FIG. 5 (color online). Variation of m_X with s_0 and M_B^2 corresponding to the current J_1 for the $0^+ sc\bar{s}\,\bar{b}$ system.

window is determined as 6.6 GeV$^2 \leq M_B^2 \leq 8.1$ GeV^2, which is much broader than the corresponding $qc\bar{q}\,\bar{b}$ system for the same current J_1. In the expressions (A10)–(A17), the order m_s parts in the perturbative and quark condensate terms have opposite signs, enhancing the strange quark contributions and resulting in a smaller lower bound on M_B^2. This is the reason that the OPE convergence of the $sc\bar{s}\,\bar{b}$ system is better than that of the $qc\bar{q}\,\bar{b}$ system.

We collect the numerical results for the scalar and axial vector $qc\bar{q}\,\bar{b}$ systems in Tables III and IV respectively, including the continuum threshold values, the Borel windows, the extracted masses and the pole contributions.

As mentioned above, the pole contributions of these $qc\bar{q}\,\bar{b}$ and $sc\bar{s}\,\bar{b}$ systems are very small making it difficult to obtain a significant Borel window. To improve the pole contribution and sum rule reliability, one possible way is using the mixed interpolating currents to calculate the spectral densities and correlation functions [5]. For both the $J^P = 0^+$ and $1^+ qc\bar{q}\,\bar{b}$ systems, J_1 and J_3 have similar Lorentz structures, which result in very similar spectral densities in the Appendix. The same situation exists for J_2 and J_4. So the reasonable choice is mixing J_1 with J_2 and mixing J_3 with J_4. However, these two mixed currents will also give the similar results due to their Lorentz structures. We therefore consider the following mixed currents:

$$J^m = \cos\theta J_1 + \sin\theta J_2, \tag{22}$$

for $J^P = 0^+ qc\bar{q}\,\bar{b}$ system and

$$J^m_\mu = \cos\theta J_{1\mu} + \sin\theta J_{2\mu}, \tag{23}$$

for $J^P = 1^+ qc\bar{q}\,\bar{b}$ system.

For J^m and J^m_μ, we just need to calculate the mixed parts $\langle 0|T[J_1 J_2^\dagger]|0\rangle + \langle 0|T[J_2 J_1^\dagger]|0\rangle$ and $\langle 0|T[J_{1\mu} J_{2\nu}^\dagger]|0\rangle + \langle 0|T[J_{2\mu} J_{1\nu}^\dagger]|0\rangle$ in the correlation functions. In the Appendix, we list the spectral densities of these two mixed parts. In these expressions, the perturbative terms, the quark condensate and the four quark condensate give no contributions to the correlation functions. Utilizing these results and the spectral densities for $J_{1\mu}$ and $J_{2\mu}$, we perform the numerical analysis in the axial vector $qc\bar{q}\,\bar{b}$

TABLE III. The threshold value, Borel window, mass and pole contribution for $J^P = 0^+ qc\bar{q}\,\bar{b}$ and $sc\bar{s}\,\bar{b}$ systems.

System	Current	s_0 (GeV^2)	$[M^2_{\rm min}, M^2_{\rm max}]$ (GeV^2)	m_X (GeV)	PC (%)
$qc\bar{q}\,\bar{b}$	J_1	55 ± 2	7.8–8.0	$7.11 \pm 0.08 \pm 0.06 \pm 0.01$	10.2
$sc\bar{s}\,\bar{b}$	J_1	56 ± 2	6.6–8.1	$7.16 \pm 0.08 \pm 0.06 \pm 0.04$	14.4
	J_2	56 ± 2	8.8–9.2	$7.10 \pm 0.09 \pm 0.04 \pm 0.13$	10.6
	J_4	56 ± 2	8.8–9.1	$7.10 \pm 0.09 \pm 0.06 \pm 0.12$	10.9

TABLE IV. The threshold value, Borel window, mass and pole contribution for $J^P = 1^+ qc\bar{q}\,\bar{b}$ and $sc\bar{s}\,\bar{b}$ systems.

System	Current	s_0(GeV^2)	$[M^2_{\rm min}, M^2_{\rm max}]$ (GeV^2)	m_X (GeV)	PC (%)
$qc\bar{q}\,\bar{b}$	$J_{1\mu}$	55 ± 2	7.9–8.2	$7.10 \pm 0.09 \pm 0.06 \pm 0.01$	10.4
	$J_{2\mu}$	55 ± 2	7.9–8.2	$7.09 \pm 0.09 \pm 0.06 \pm 0.01$	10.7
$sc\bar{s}\,\bar{b}$	$J_{1\mu}$	55 ± 2	6.7–7.9	$7.11 \pm 0.08 \pm 0.05 \pm 0.03$	14.0
	$J_{2\mu}$	56 ± 2	6.7–8.3	$7.15 \pm 0.09 \pm 0.06 \pm 0.05$	14.2
	$J_{3\mu}$	52 ± 2	6.7–7.3	$6.90 \pm 0.09 \pm 0.02 \pm 0.03$	11.6
	$J_{4\mu}$	52 ± 2	6.7–7.3	$6.92 \pm 0.09 \pm 0.06 \pm 0.03$	11.0

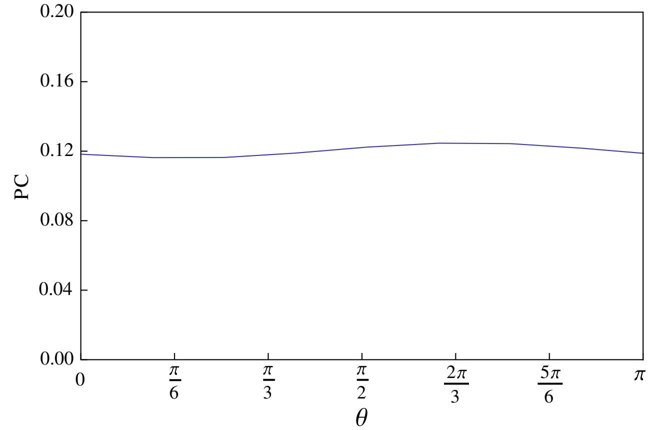

FIG. 6 (color online). Pole contribution as a function of the mixing angle θ with $s_0 = 55\ \mathrm{GeV}^2$ and $M_B^2 = 8.0\ \mathrm{GeV}^2$ for J_μ^m.

channel with the mixed current J_μ^m. Under the same criteria of the OPE convergence and pole contribution, we obtain the Borel window $7.9\ \mathrm{GeV}^2 \le M_B^2 \le 8.4\ \mathrm{GeV}^2$ with $s_0 = 55\ \mathrm{GeV}^2$. To study the mixing effect, we show the variation of the pole contribution with the mixing angle θ in Fig. 6. It shows that there is no significant enhancement of the pole contribution for all the values of mixing angles. In Fig. 7, we show the Borel curves of the extracted mass with s_0 and M_B^2 for the $J^P = 1^+ qc\bar{q}\,\bar{b}$ system with the mixed current J_μ^m. Finally, we extract the ground state mass around 7.11 GeV. Compared to the numerical results from the single current in Table IV, the mass, continuum threshold, Borel window and pole contribution from the mixed current J_μ^m are almost the same. The similar situation occurs for the mixed current J^m. In other words, the mixed current does not improve the mass sum rules significantly.

V. SUMMARY

We have constructed the $bc\bar{q}\,\bar{q}$, $bc\bar{s}\,\bar{s}$ and $qc\bar{q}\,\bar{b}$, $sc\bar{s}\,\bar{b}$ tetraquark currents with $J^P = 0^+$ and 1^+. At the leading order in α_s, we calculate the two-point correlation functions and the spectral densities including the contributions of the perturbative terms, quark condensate $\langle\bar{q}q\rangle$, gluon condensate $\langle GG\rangle$, quark-gluon mixed condensate $\langle\bar{q}g_s\sigma\cdot Gq\rangle$, four quark condensate $\langle\bar{q}q\rangle^2$ and dimension eight condensate $\langle\bar{q}q\rangle\langle\bar{q}g_s\sigma\cdot Gq\rangle$.

For the $bc\bar{q}\,\bar{q}$ systems, both the quark condensate $\langle\bar{q}q\rangle$ and quark-gluon mixed condensate $\langle\bar{q}g_s\sigma\cdot Gq\rangle$ are proportional to the light quark mass m_q and vanish in the chiral limit $m_q = 0$. The four quark condensate $\langle\bar{q}q\rangle^2$ is the dominant power correction to the correlation functions. The dimension eight condensate $\langle\bar{q}q\rangle\langle\bar{q}g_s\sigma\cdot Gq\rangle$ also gives an important contribution. To study the $bc\bar{s}\,\bar{s}$ systems, we keep the leading-order m_s corrections to the spectral densities. The numerical analysis shows that these terms can improve the OPE convergence and pole contribution to enlarge the Borel window of the mass sum rules. The extracted masses for both the scalar and axial vector $bc\bar{q}\,\bar{q}$ and $bc\bar{s}\,\bar{s}$ tetraquark states are about $7.1 - 7.2$ GeV and $7.2 - 7.3$ GeV, respectively.

The situation for the $qc\bar{q}\,\bar{b}$ systems is very different from that of the $bc\bar{q}\,\bar{q}$ systems. The quark condensate $\langle\bar{q}q\rangle$ and quark-gluon mixed condensate $\langle\bar{q}g_s\sigma\cdot Gq\rangle$ are multiplied by the heavy quark mass m_Q and give important contributions to the correlation functions. The quark condensate is the dominant power correction in these systems. After performing the numerical analysis, we extract the masses of both the scalar and axial vector $qc\bar{q}\,\bar{b}$ states around 7.1 GeV. The mass is about 7.1 GeV for the scalar $sc\bar{s}\,\bar{b}$ state and $6.9 - 7.1$ GeV for the axial vector $sc\bar{s}\,\bar{b}$ state. However, the pole contributions of these $qc\bar{q}\,\bar{b}$ systems are so small that the corresponding Borel windows are very narrow. To improve the pole contributions and enlarge the Borel windows, we investigated the mixed interpolating currents by introducing a mixing angle θ. Unfortunately, the numerical analysis shows that these mixed currents give no significant effects that would expand the Borel window.

The masses of these $bc\bar{q}\,\bar{q}$, $bc\bar{s}\,\bar{s}$ and $qc\bar{q}\,\bar{b}$, $sc\bar{s}\,\bar{b}$ tetraquark states are below the open-flavor thresholds $D^{(*)}\bar{B}^{(*)}$, $D_s^{(*)}\bar{B}_s^{(*)}$ and $D^{(*)}B^{(*)}$, $D_s^{(*)}B_s^{(*)}$, respectively. In other words, these tetraquark states $bc\bar{q}\,\bar{q}$, $bc\bar{s}\,\bar{s}$ and $qc\bar{q}\,\bar{b}$, $sc\bar{s}\,\bar{b}$ cannot decay into the open-flavor modes due to the

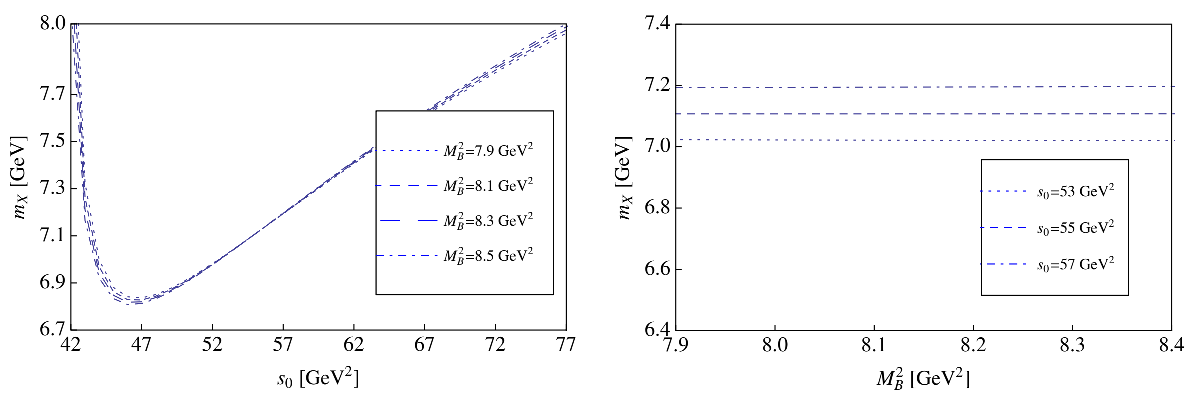

FIG. 7 (color online). Variation of m_X with s_0 and M_B^2 corresponding to the mixed current J_μ^m for the $1^+ qc\bar{q}\,\bar{b}$ system.

kinematics limits. On the other hand, the B_c plus light meson decay modes for the $qc\bar{q}\,\bar{b}$ states are allowed, such as $X(0^+) \to B_c\pi, B_c\eta$ and $X(1^+) \to B_c\rho, B_c\omega$. Such channels are suggested for the future search of these possible $qc\bar{q}\,\bar{b}$, $sc\bar{s}\,\bar{b}$ states. The $bc\bar{q}\,\bar{q}$ and $bc\bar{s}\,\bar{s}$ tetraquark states cannot decay through these fall-apart mechanisms, suggesting dominantly weak decay mechanisms. They may be produced at facilities such as Super-B factories, LHCb, PANDA and RHIC.

ACKNOWLEDGMENTS

This project was supported by the Natural Sciences and Engineering Research Council of Canada (NSERC). S. L. Z. was supported by the National Natural Science Foundation of China under Grant No. 11261130311.

APPENDIX: SPECTRAL DENSITIES

In this Appendix, we list the spectral densities of the tetraquark interpolating currents in Eqs. (1)–(4). At leading order in α_s, we calculate the spectral densities including the perturbative terms, quark condensate $\langle\bar{q}q\rangle$, gluon condensate $\langle GG\rangle$, quark-gluon mixed condensate $\langle\bar{q}g_s\sigma\cdot Gq\rangle$ and dimension eight condensate $\langle\bar{q}q\rangle\langle\bar{q}g_s\sigma\cdot Gq\rangle$:

$$\rho(s) = \rho^{\rm pert}(s) + \rho^{\langle\bar{q}q\rangle}(s) + \rho^{\langle GG\rangle}(s) + \rho^{\langle\bar{q}Gq\rangle}(s) + \rho^{\langle\bar{q}q\rangle^2}(s) + \rho^{\langle\bar{q}q\rangle\langle\bar{q}Gq\rangle}(s). \tag{A1}$$

1. The spectral densities for the $bc\bar{q}\,\bar{q}$ and $bc\bar{s}\,\bar{s}$ systems

For the interpolating current J_1 with $J^P = 0^+$:

$$\begin{aligned}
\rho_1^{\rm pert}(s) &= \int_{\alpha_{\rm min}}^{\alpha_{\rm max}} d\alpha \int_{\beta_{\rm min}}^{\beta_{\rm max}} d\beta \frac{(1-\alpha-\beta)^2(m_1^2\beta+m_2^2\alpha-\alpha\beta s)^3(m_1^2\beta+m_2^2\alpha-3\alpha\beta s-2m_1m_2)}{256\pi^6\alpha^3\beta^3},\\
\rho_1^{\langle\bar{q}q\rangle}(s) &= -m_q\langle\bar{q}q\rangle \int_{\alpha_{\rm min}}^{\alpha_{\rm max}} d\alpha \int_{\beta_{\rm min}}^{\beta_{\rm max}} d\beta \frac{(m_1^2\beta+m_2^2\alpha-\alpha\beta s)(m_1^2\beta+m_2^2\alpha-2\alpha\beta s-m_1m_2)}{8\pi^4\alpha\beta},\\
\rho_{1a}^{\langle GG\rangle}(s) &= \langle g_s^2GG\rangle \int_{\alpha_{\rm min}}^{\alpha_{\rm max}} d\alpha \int_{\beta_{\rm min}}^{\beta_{\rm max}} d\beta \frac{(1-\alpha-\beta)^2}{1536\pi^6}\left[(2m_1^2\beta+2m_2^2\alpha-3\alpha\beta s)\left(\frac{m_1^2}{\alpha^3}+\frac{m_2^2}{\beta^3}\right)\right.\\
&\quad\left.-\frac{m_1m_2}{\alpha\beta}\left(\frac{4m_1^2\beta+3m_2^2\alpha-3\alpha\beta s}{\alpha^2}+\frac{3m_1^2\beta+4m_2^2\alpha-3\alpha\beta s}{\beta^2}\right)\right],\\
\rho_{1b}^{\langle GG\rangle}(s) &= -\langle g_s^2GG\rangle \int_{\alpha_{\rm min}}^{\alpha_{\rm max}} d\alpha \int_{\beta_{\rm min}}^{\beta_{\rm max}} d\beta \frac{(m_1^2\beta+m_2^2\alpha-\alpha\beta s)}{1024\pi^6}\\
&\quad\times\left[\frac{m_1^2\beta+m_2^2\alpha-2\alpha\beta s-m_1m_2}{\alpha\beta}+\frac{(1-\alpha-\beta)^2(m_1^2\beta+m_2^2\alpha-2\alpha\beta s-2m_1m_2)}{2\alpha^2\beta^2}\right],\\
\rho_1^{\langle\bar{q}Gq\rangle}(s) &= -\frac{m_q\langle\bar{q}g_s\sigma\cdot Gq\rangle[s-(m_1-m_2)^2]}{32\pi^4}\left[\left(1+\frac{m_1^2-m_2^2}{s}\right)^2-\frac{4m_1^2}{s}\right]^{1/2},\\
\rho_1^{\langle\bar{q}q\rangle^2}(s) &= \frac{\langle\bar{q}q\rangle^2[s-(m_1-m_2)^2]}{12\pi^2}\left[\left(1+\frac{m_1^2-m_2^2}{s}\right)^2-\frac{4m_1^2}{s}\right]^{1/2},\\
\rho_1^{\langle\bar{q}q\rangle\langle\bar{q}Gq\rangle}(s) &= -\frac{\langle\bar{q}q\rangle\langle\bar{q}Gq\rangle}{12\pi^2}\int_0^1 d\alpha\left\{\left[\frac{m_2^4-m_1m_2^3}{\alpha^2}-\frac{m_2^4(1-\alpha)+m_1^2m_2^2\alpha}{\alpha^2(1-\alpha)}\right]\delta'\left[s-\frac{m_1^2\alpha+m_2^2(1-\alpha)}{\alpha(1-\alpha)}\right]\right.\\
&\quad\left.-\frac{m_1^2\alpha+m_2^2(1-\alpha)}{\alpha(1-\alpha)}\delta\left[s-\frac{m_1^2\alpha+m_2^2(1-\alpha)}{\alpha(1-\alpha)}\right]-H\left[s-\frac{m_1^2\alpha+m_2^2(1-\alpha)}{\alpha(1-\alpha)}\right]\right\},
\end{aligned}\tag{A2}$$

where $\alpha_{\rm min} = \frac{1}{2}\{1+\frac{m_1^2-m_2^2}{s}-[(1+\frac{m_1^2-m_2^2}{s})^2-\frac{4m_1^2}{s}]^{1/2}\}$, $\alpha_{\rm max} = \frac{1}{2}\{1+\frac{m_1^2-m_2^2}{s}+[(1+\frac{m_1^2-m_2^2}{s})^2-\frac{4m_1^2}{s}]^{1/2}\}$, $\beta_{\rm min} = \frac{\alpha m_2^2}{\alpha s-m_1^2}$, $\beta_{\rm max} = 1-\alpha$. m_1 and m_2 are the heavy quark masses. $H(\alpha)$ is the Heaviside step function.

For the interpolating current J_3 with $J^P = 0^+$:

$$\begin{aligned}
&\rho_3^{\rm pert}(s) = \frac{1}{2}\rho_1^{\rm pert}(s), \qquad \rho_3^{\langle\bar{q}q\rangle}(s) = \frac{1}{2}\rho_1^{\langle\bar{q}q\rangle}(s), \qquad \rho_{3a}^{\langle GG\rangle}(s) = \frac{1}{2}\rho_{1a}^{\langle GG\rangle}(s), \qquad \rho_{3b}^{\langle GG\rangle}(s) = -\rho_{1b}^{\langle GG\rangle}(s),\\
&\rho_3^{\langle\bar{q}Gq\rangle}(s) = \frac{1}{2}\rho_1^{\langle\bar{q}Gq\rangle}(s), \qquad \rho_3^{\langle\bar{q}q\rangle^2}(s) = \frac{1}{2}\rho_1^{\langle\bar{q}q\rangle^2}(s), \qquad \rho_3^{\langle\bar{q}q\rangle\langle\bar{q}Gq\rangle}(s) = \frac{1}{2}\rho_1^{\langle\bar{q}q\rangle\langle\bar{q}Gq\rangle}(s).
\end{aligned}\tag{A3}$$

For the interpolating current J_2 with $J^P = 0^+$:

$$\rho_2^{\mathrm{pert}}(s) = \int_{\alpha_{\min}}^{\alpha_{\max}} d\alpha \int_{\beta_{\min}}^{\beta_{\max}} d\beta \frac{(1-\alpha-\beta)^2(m_1^2\beta+m_2^2\alpha-\alpha\beta s)^3(m_1^2\beta+m_2^2\alpha-3\alpha\beta s-4m_1m_2)}{64\pi^6\alpha^3\beta^3},$$

$$\rho_2^{\langle\bar{q}q\rangle}(s) = -m_q\langle\bar{q}q\rangle \int_{\alpha_{\min}}^{\alpha_{\max}} d\alpha \int_{\beta_{\min}}^{\beta_{\max}} d\beta \frac{3(m_1^2\beta+m_2^2\alpha-\alpha\beta s)(m_1^2\beta+m_2^2\alpha-2\alpha\beta s-2m_1m_2)}{2\pi^4\alpha\beta},$$

$$\rho_{2a}^{\langle GG\rangle}(s) = \langle g_s^2GG\rangle \int_{\alpha_{\min}}^{\alpha_{\max}} d\alpha \int_{\beta_{\min}}^{\beta_{\max}} d\beta \frac{(1-\alpha-\beta)^2}{384\pi^6}\left[(2m_1^2\beta+2m_2^2\alpha-3\alpha\beta s)\left(\frac{m_1^2}{\alpha^3}+\frac{m_2^2}{\beta^3}\right)\right.$$
$$\left.-\frac{2m_1m_2}{\alpha\beta}\left(\frac{4m_1^2\beta+3m_2^2\alpha-3\alpha\beta s}{\alpha^2}+\frac{3m_1^2\beta+4m_2^2\alpha-3\alpha\beta s}{\beta^2}\right)\right],$$

$$\rho_{2b}^{\langle GG\rangle}(s) = \langle g_s^2GG\rangle \int_{\alpha_{\min}}^{\alpha_{\max}} d\alpha \int_{\beta_{\min}}^{\beta_{\max}} d\beta \frac{(m_1^2\beta+m_2^2\alpha-\alpha\beta s)}{256\pi^6}$$
$$\times\left[\frac{m_1^2\beta+m_2^2\alpha-2\alpha\beta s-2m_1m_2}{\alpha\beta}+\frac{(1-\alpha-\beta)^2(m_1^2\beta+m_2^2\alpha-2\alpha\beta s)}{2\alpha^2\beta^2}\right],$$

$$\rho_2^{\langle\bar{q}Gq\rangle}(s) = -\frac{m_q\langle\bar{q}g_s\sigma\cdot Gq\rangle[s-(m_1-m_2)^2+2m_1m_2]}{4\pi^4}\left[\left(1+\frac{m_1^2-m_2^2}{s}\right)^2-\frac{4m_1^2}{s}\right]^{1/2},$$

$$\rho_2^{\langle\bar{q}q\rangle^2}(s) = \frac{2\langle\bar{q}q\rangle^2[s-(m_1-m_2)^2+2m_1m_2]}{3\pi^2}\left[\left(1+\frac{m_1^2-m_2^2}{s}\right)^2-\frac{4m_1^2}{s}\right]^{1/2},$$

$$\rho_2^{\langle\bar{q}q\rangle\langle\bar{q}Gq\rangle}(s) = -\frac{2\langle\bar{q}q\rangle\langle\bar{q}Gq\rangle}{3\pi^2}\int_0^1 d\alpha\left\{\left[\frac{m_2^4-2m_1m_2^3}{\alpha^2}-\frac{m_2^4(1-\alpha)+m_1^2m_2^2\alpha}{\alpha^2(1-\alpha)}\right]\delta'\left[s-\frac{m_1^2\alpha+m_2^2(1-\alpha)}{\alpha(1-\alpha)}\right]\right.$$
$$\left.-\frac{m_1^2\alpha+m_2^2(1-\alpha)}{\alpha(1-\alpha)}\delta\left[s-\frac{m_1^2\alpha+m_2^2(1-\alpha)}{\alpha(1-\alpha)}\right]-H\left[s-\frac{m_1^2\alpha+m_2^2(1-\alpha)}{\alpha(1-\alpha)}\right]\right\}. \tag{A4}$$

For the interpolating current J_4 with $J^P = 0^+$:

$$\rho_4^{\mathrm{pert}}(s)=\frac{1}{2}\rho_2^{\mathrm{pert}}(s),\qquad \rho_4^{\langle\bar{q}q\rangle}(s)=\frac{1}{2}\rho_2^{\langle\bar{q}q\rangle}(s),\qquad \rho_{4a}^{\langle GG\rangle}(s)=\frac{1}{2}\rho_{2a}^{\langle GG\rangle}(s),\qquad \rho_{4b}^{\langle GG\rangle}(s)=-\rho_{2b}^{\langle GG\rangle}(s),$$
$$\rho_4^{\langle\bar{q}Gq\rangle}(s)=\frac{1}{2}\rho_2^{\langle\bar{q}Gq\rangle}(s),\qquad \rho_4^{\langle\bar{q}q\rangle^2}(s)=\frac{1}{2}\rho_2^{\langle\bar{q}q\rangle^2}(s),\qquad \rho_4^{\langle\bar{q}q\rangle\langle\bar{q}Gq\rangle}(s)=\frac{1}{2}\rho_2^{\langle\bar{q}q\rangle\langle\bar{q}Gq\rangle}(s). \tag{A5}$$

For the interpolating current J_1 with $J^P = 1^+$:

$$\rho_1^{\mathrm{pert}}(s) = \int_{\alpha_{\min}}^{\alpha_{\max}} d\alpha \int_{\beta_{\min}}^{\beta_{\max}} d\beta \frac{(1-\alpha-\beta)^2(m_1^2\beta+m_2^2\alpha-\alpha\beta s)^3}{1536\pi^6\alpha^3\beta^3}$$
$$\times[6(m_1^2\beta+m_2^2\alpha-3\alpha\beta s-2m_1m_2)-(1-\alpha-\beta)(3m_1^2\beta+3m_2^2\alpha-7\alpha\beta s-4m_1m_2)],$$

$$\rho_1^{\langle\bar{q}q\rangle}(s) = -\frac{m_q\langle\bar{q}q\rangle}{16\pi^4}\int_{\alpha_{\min}}^{\alpha_{\max}} d\alpha \int_{\beta_{\min}}^{\beta_{\max}} d\beta \frac{(m_1^2\beta+m_2^2\alpha-\alpha\beta s)}{\alpha\beta}$$
$$\times[2(m_1^2\beta+m_2^2\alpha-2\alpha\beta s-m_1m_2)-(1-\alpha-\beta)(3m_1^2\beta+3m_2^2\alpha-5\alpha\beta s-2m_1m_2)],$$

$$\rho_{1a}^{\langle GG\rangle}(s) = \langle g_s^2GG\rangle \int_{\alpha_{\min}}^{\alpha_{\max}} d\alpha \int_{\beta_{\min}}^{\beta_{\max}} d\beta \frac{(1-\alpha-\beta)^2}{4608\pi^6}$$
$$\times\left\{\left(\frac{m_1^2}{\alpha^3}+\frac{m_2^2}{\beta^3}\right)[3(2m_1^2\beta+2m_2^2\alpha-3\alpha\beta s)-(1-\alpha-\beta)(3m_1^2\beta+3m_2^2\alpha-4\alpha\beta s)]\right.$$
$$\left.-\frac{m_1m_2(2+\alpha+\beta)}{\alpha\beta}\left(\frac{4m_1^2\beta+3m_2^2\alpha-3\alpha\beta s}{\alpha^2}+\frac{3m_1^2\beta+4m_2^2\alpha-3\alpha\beta s}{\beta^2}\right)\right\},$$

$$
\begin{aligned}
\rho_{1b}^{\langle GG\rangle}(s) &= \langle g_s^2GG\rangle \int_{\alpha_{\min}}^{\alpha_{\max}} d\alpha \int_{\beta_{\min}}^{\beta_{\max}} d\beta \frac{(m_1^2\beta + m_2^2\alpha - \alpha\beta s)}{12288\pi^6}\Bigg\{(1-\alpha-\beta)^2 \\
&\quad \times \left[\frac{(1-\alpha-\beta)(3m_1^2\beta + 3m_2^2\alpha - 5\alpha\beta s - 4m_1m_2)}{\alpha^2\beta^2} - \frac{6(m_1^2\beta + m_2^2\alpha - 2\alpha\beta s - 2m_1m_2)}{\alpha^2\beta^2}\right] \\
&\quad + \left[\frac{2(1-\alpha-\beta)(3m_1^2\beta + 3m_2^2\alpha - 5\alpha\beta s - 2m_1m_2)}{\alpha\beta} + \frac{4(m_1^2\beta + m_2^2\alpha - 2\alpha\beta s - m_1m_2)}{\alpha\beta}\right]\Bigg\}, \\
\rho_1^{\langle\bar{q}Gq\rangle}(s) &= -\frac{m_q\langle\bar{q}g_s\sigma\cdot Gq\rangle[s-(m_1-m_2)^2]}{32\pi^4}\left[\left(1+\frac{m_1^2-m_2^2}{s}\right)^2 - \frac{4m_1^2}{s}\right]^{1/2}, \\
\rho_1^{\langle\bar{q}q\rangle^2}(s) &= \frac{\langle\bar{q}q\rangle^2[s-(m_1-m_2)^2]}{12\pi^2}\left[\left(1+\frac{m_1^2-m_2^2}{s}\right)^2 - \frac{4m_1^2}{s}\right]^{1/2}, \\
\rho_1^{\langle\bar{q}q\rangle\langle\bar{q}Gq\rangle}(s) &= -\frac{\langle\bar{q}q\rangle\langle\bar{q}Gq\rangle}{12\pi^2}\int_0^1 d\alpha\Bigg\{\left[\frac{m_2^4 - m_1m_2^3}{\alpha^2} - \frac{m_2^4(1-\alpha) + m_1^2m_2^2\alpha}{\alpha^2(1-\alpha)}\right]\delta'\left[s - \frac{m_1^2\alpha + m_2^2(1-\alpha)}{\alpha(1-\alpha)}\right] \\
&\quad - \frac{m_1^2\alpha + m_2^2(1-\alpha)}{\alpha(1-\alpha)}\delta\left[s - \frac{m_1^2\alpha + m_2^2(1-\alpha)}{\alpha(1-\alpha)}\right] - H\left[s - \frac{m_1^2\alpha + m_2^2(1-\alpha)}{\alpha(1-\alpha)}\right]\Bigg\}. \qquad \text{(A6)}
\end{aligned}
$$

For the interpolating current J_3 with $J^P = 1^+$:

$$
\begin{aligned}
&\rho_3^{\mathrm{pert}}(s) = \frac{1}{2}\rho_1^{\mathrm{pert}}(s), \qquad \rho_3^{\langle\bar{q}q\rangle}(s) = \frac{1}{2}\rho_1^{\langle\bar{q}q\rangle}(s), \qquad \rho_{3a}^{\langle GG\rangle}(s) = \frac{1}{2}\rho_{1a}^{\langle GG\rangle}(s), \qquad \rho_{3b}^{\langle GG\rangle}(s) = -\rho_{1b}^{\langle GG\rangle}(s), \\
&\rho_3^{\langle\bar{q}Gq\rangle}(s) = \frac{1}{2}\rho_1^{\langle\bar{q}Gq\rangle}(s), \qquad \rho_3^{\langle\bar{q}q\rangle^2}(s) = \frac{1}{2}\rho_1^{\langle\bar{q}q\rangle^2}(s), \qquad \rho_3^{\langle\bar{q}q\rangle\langle\bar{q}Gq\rangle}(s) = \frac{1}{2}\rho_1^{\langle\bar{q}q\rangle\langle\bar{q}Gq\rangle}(s). \qquad \text{(A7)}
\end{aligned}
$$

For the interpolating current J_2 with $J^P = 1^+$:

$$
\begin{aligned}
\rho_2^{\mathrm{pert}}(s) &= \int_{\alpha_{\min}}^{\alpha_{\max}} d\alpha \int_{\beta_{\min}}^{\beta_{\max}} d\beta \frac{(1-\alpha-\beta)^2(m_1^2\beta + m_2^2\alpha - \alpha\beta s)^3(m_1^2\beta + m_2^2\alpha - 5\alpha\beta s - 4m_1m_2)}{512\pi^6\alpha^3\beta^3}, \\
\rho_2^{\langle\bar{q}q\rangle}(s) &= -m_q\langle\bar{q}q\rangle \int_{\alpha_{\min}}^{\alpha_{\max}} d\alpha \int_{\beta_{\min}}^{\beta_{\max}} d\beta \frac{(m_1^2\beta + m_2^2\alpha - \alpha\beta s)(m_1^2\beta + m_2^2\alpha - 3\alpha\beta s - 2m_1m_2)}{16\pi^4\alpha\beta}, \\
\rho_{2a}^{\langle GG\rangle}(s) &= \langle g_s^2GG\rangle \int_{\alpha_{\min}}^{\alpha_{\max}} d\alpha \int_{\beta_{\min}}^{\beta_{\max}} d\beta \frac{(1-\alpha-\beta)^2}{1536\pi^6}\Bigg[(m_1^2\beta + m_2^2\alpha - 2\alpha\beta s)\left(\frac{m_1^2}{\alpha^3} + \frac{m_2^2}{\beta^3}\right) \\
&\quad - \frac{m_1m_2}{\alpha\beta}\left(\frac{4m_1^2\beta + 3m_2^2\alpha - 3\alpha\beta s}{\alpha^2} + \frac{3m_1^2\beta + 4m_2^2\alpha - 3\alpha\beta s}{\beta^2}\right)\Bigg], \\
\rho_{2b}^{\langle GG\rangle}(s) &= -\langle g_s^2GG\rangle \int_{\alpha_{\min}}^{\alpha_{\max}} d\alpha \int_{\beta_{\min}}^{\beta_{\max}} d\beta \frac{(m_1^2\beta + m_2^2\alpha - \alpha\beta s)}{12288\pi^6} \\
&\quad \times \left[\frac{6(m_1^2\beta + m_2^2\alpha - 3\alpha\beta s - 2m_1m_2)}{\alpha\beta} - \frac{(1-\alpha-\beta)^2(3m_1^2\beta + 3m_2^2\alpha - 5\alpha\beta s)}{\alpha^2\beta^2}\right], \\
\rho_2^{\langle\bar{q}Gq\rangle}(s) &= -\frac{m_q\langle\bar{q}g_s\sigma\cdot Gq\rangle[2s^2 - (m_1^2 - 6m_1m_2 + m_2^2)s - (m_1^2-m_2^2)^2]}{96\pi^4 s}\left[\left(1+\frac{m_1^2-m_2^2}{s}\right)^2 - \frac{4m_1^2}{s}\right]^{1/2}, \\
\rho_2^{\langle\bar{q}q\rangle^2}(s) &= \frac{\langle\bar{q}q\rangle^2[2s^2 - (m_1^2 - 6m_1m_2 + m_2^2)s - (m_1^2-m_2^2)^2]}{36\pi^2 s}\left[\left(1+\frac{m_1^2-m_2^2}{s}\right)^2 - \frac{4m_1^2}{s}\right]^{1/2}, \\
\rho_2^{\langle\bar{q}q\rangle\langle\bar{q}Gq\rangle}(s) &= -\frac{\langle\bar{q}q\rangle\langle\bar{q}Gq\rangle}{12\pi^2}\int_0^1 d\alpha\Bigg\{\left[\frac{m_2^4 - m_1m_2^3}{\alpha^2} - \frac{m_2^4(1-\alpha) + m_1^2m_2^2\alpha}{\alpha^2(1-\alpha)}\right]\delta'\left[s - \frac{m_1^2\alpha + m_2^2(1-\alpha)}{\alpha(1-\alpha)}\right] \\
&\quad - \frac{m_1^2\alpha + m_2^2(1-\alpha)}{\alpha(1-\alpha)}\delta\left[s - \frac{m_1^2\alpha + m_2^2(1-\alpha)}{\alpha(1-\alpha)}\right] - \alpha * H\left[s - \frac{m_1^2\alpha + m_2^2(1-\alpha)}{\alpha(1-\alpha)}\right]\Bigg\}. \qquad \text{(A8)}
\end{aligned}
$$

For the interpolating current J_4 with $J^P = 1^+$:

$$\rho_4^{\rm pert}(s) = \frac{1}{2}\rho_2^{\rm pert}(s), \qquad \rho_4^{\langle\bar{q}q\rangle}(s) = \frac{1}{2}\rho_2^{\langle\bar{q}q\rangle}(s), \qquad \rho_{4a}^{\langle GG\rangle}(s) = \frac{1}{2}\rho_{2a}^{\langle GG\rangle}(s), \qquad \rho_{4b}^{\langle GG\rangle}(s) = -\rho_{2b}^{\langle GG\rangle}(s),$$
$$\rho_4^{\langle\bar{q}Gq\rangle}(s) = \frac{1}{2}\rho_2^{\langle\bar{q}Gq\rangle}(s), \qquad \rho_4^{\langle\bar{q}q\rangle^2}(s) = \frac{1}{2}\rho_2^{\langle\bar{q}q\rangle^2}(s), \qquad \rho_4^{\langle\bar{q}q\rangle\langle\bar{q}Gq\rangle}(s) = \frac{1}{2}\rho_2^{\langle\bar{q}q\rangle\langle\bar{q}Gq\rangle}(s). \tag{A9}$$

2. The spectral densities for the $qc\bar{q}\bar{b}$ and $sc\bar{s}\bar{b}$ systems

For the interpolating current J_1 with $J^P = 0^+$:

$$\begin{aligned}
\rho_1^{\rm pert}(s) &= \int_{\alpha_{\rm min}}^{\alpha_{\rm max}} d\alpha \int_{\beta_{\rm min}}^{\beta_{\rm max}} d\beta \frac{(1-\alpha-\beta)^2(m_1^2\beta + m_2^2\alpha - \alpha\beta s)^2}{256\pi^6} \\
&\quad\times \left[\frac{(m_1^2\beta + m_2^2\alpha - 3\alpha\beta s)(m_1^2\beta + m_2^2\alpha - \alpha\beta s)}{\alpha^3\beta^3} - \left(\frac{m_1}{\alpha} + \frac{m_2}{\beta}\right)\frac{2m_q(2m_1^2\beta + 2m_2^2\alpha - 5\alpha\beta s)}{\alpha^2\beta^2}\right], \\
\rho_1^{\langle\bar{q}q\rangle}(s) &= \langle\bar{q}q\rangle \int_{\alpha_{\rm min}}^{\alpha_{\rm max}} d\alpha \int_{\beta_{\rm min}}^{\beta_{\rm max}} d\beta \frac{(m_1^2\beta + m_2^2\alpha - \alpha\beta s)}{8\pi^4\alpha\beta} \\
&\quad\times \left[m_q(m_1^2\beta + m_2^2\alpha - 2\alpha\beta s + 2m_1m_2) - \left(\frac{m_1}{\alpha} + \frac{m_2}{\beta}\right)(1-\alpha-\beta)(m_1^2\beta + m_2^2\alpha - 2\alpha\beta s)\right], \\
\rho_{1a}^{\langle GG\rangle}(s) &= \langle g_s^2 GG\rangle \int_{\alpha_{\rm min}}^{\alpha_{\rm max}} d\alpha \int_{\beta_{\rm min}}^{\beta_{\rm max}} d\beta \frac{(1-\alpha-\beta)^2(2m_1^2\beta + 2m_2^2\alpha - 3\alpha\beta s)}{1536\pi^6}\left(\frac{m_1^2}{\alpha^3} + \frac{m_2^2}{\beta^3}\right), \\
\rho_{1b}^{\langle GG\rangle}(s) &= -\langle g_s^2 GG\rangle \int_{\alpha_{\rm min}}^{\alpha_{\rm max}} d\alpha \int_{\beta_{\rm min}}^{\beta_{\rm max}} d\beta \frac{(1-\alpha-\beta)(m_1^2\beta + m_2^2\alpha - 2\alpha\beta s)(m_1^2\beta + m_2^2\alpha - \alpha\beta s)}{1024\pi^6\alpha\beta}\left(\frac{1}{\alpha} + \frac{1}{\beta}\right), \\
\rho_{1a}^{\langle\bar{q}Gq\rangle}(s) &= \langle\bar{q}g_s\sigma\cdot Gq\rangle \int_{\alpha_{\rm min}}^{\alpha_{\rm max}} d\alpha \int_{\beta_{\rm min}}^{\beta_{\rm max}} d\beta \frac{(2m_1^2\beta + 2m_2^2\alpha - 3\alpha\beta s)}{32\pi^4}\left(\frac{m_1}{\alpha} + \frac{m_2}{\beta}\right), \\
\rho_{1b}^{\langle\bar{q}Gq\rangle}(s) &= \langle\bar{q}g_s\sigma\cdot Gq\rangle \int_{\alpha_{\rm min}}^{\alpha_{\rm max}} d\alpha \int_{\beta_{\rm min}}^{\beta_{\rm max}} d\beta \\
&\quad\times \left[\frac{(1-\alpha-\beta)(2m_1^2\beta + 2m_2^2\alpha - 3\alpha\beta s)}{64\pi^4}\left(\frac{m_1}{\alpha^2} + \frac{m_2}{\beta^2}\right) - \frac{m_qm_1m_2}{64\pi^4}\left(\frac{1}{\alpha} + \frac{1}{\beta}\right)\right], \\
\rho_{1c}^{\langle\bar{q}Gq\rangle}(s) &= -\frac{m_qm_1m_2\langle\bar{q}g_s\sigma\cdot Gq\rangle}{16\pi^4}\left[\left(1 + \frac{m_1^2 - m_2^2}{s}\right)^2 - \frac{4m_1^2}{s}\right]^{1/2}, \\
\rho_1^{\langle\bar{q}q\rangle^2}(s) &= \frac{\langle\bar{q}q\rangle^2}{12\pi^2}\left[\left(1 + \frac{m_1^2 - m_2^2}{s}\right)^2 - \frac{4m_1^2}{s}\right]^{1/2}\left\{2m_1m_2 - \frac{m_qm_1(m_1^2 - m_2^2 - s) + m_qm_2(m_1^2 - m_2^2 + s)}{s}\right. \\
&\quad + \frac{m_qm_1}{s[(m_1^2 - m_2^2 - s)^2 - 4m_2^2s]}[m_1^6 - m_2^6 + m_2^4s - m_1^4(3m_2^2 + 2s) + m_1^2(3m_2^4 + m_2^2s + s^2)] \\
&\quad \left. + \frac{m_qm_2}{s[(m_1^2 - m_2^2 - s)^2 - 4m_2^2s]}[m_1^6 - m_1^4(3m_2^2 + s) + m_1^2(3m_2^4 - m_2^2s) - (m_2^3 - m_2s)^2]\right\}, \\
\rho_{1a}^{\langle\bar{q}q\rangle\langle\bar{q}Gq\rangle}(s) &= \frac{\langle\bar{q}q\rangle\langle\bar{q}Gq\rangle}{12\pi^2}\int_0^1 d\alpha \frac{m_1m_2^3}{\alpha^2}\delta'\left[s - \frac{m_1^2\alpha + m_2^2(1-\alpha)}{\alpha(1-\alpha)}\right], \\
\rho_{1b}^{\langle\bar{q}q\rangle\langle\bar{q}Gq\rangle}(s) &= \frac{\langle\bar{q}q\rangle\langle\bar{q}Gq\rangle}{48\pi^2}\int_0^1 d\alpha \frac{m_1m_2}{\alpha(1-\alpha)}\delta\left[s - \frac{m_1^2\alpha + m_2^2(1-\alpha)}{\alpha(1-\alpha)}\right].
\end{aligned} \tag{A10}$$

For the interpolating current J_3 with $J^P = 0^+$:

$$\rho_3^{\rm pert}(s) = \frac{1}{2}\rho_1^{\rm pert}(s), \qquad \rho_3^{\langle\bar{q}q\rangle}(s) = \frac{1}{2}\rho_1^{\langle\bar{q}q\rangle}(s), \qquad \rho_{3a}^{\langle GG\rangle}(s) = \frac{1}{2}\rho_{1a}^{\langle GG\rangle}(s), \qquad \rho_{3b}^{\langle GG\rangle}(s) = -\rho_{1b}^{\langle GG\rangle}(s),$$
$$\rho_{3a}^{\langle\bar{q}Gq\rangle}(s) = \frac{1}{2}\rho_{1a}^{\langle\bar{q}Gq\rangle}(s), \qquad \rho_{3b}^{\langle\bar{q}Gq\rangle}(s) = -\rho_{1b}^{\langle\bar{q}Gq\rangle}(s), \qquad \rho_{3c}^{\langle\bar{q}Gq\rangle}(s) = \frac{1}{2}\rho_{1c}^{\langle\bar{q}Gq\rangle}(s), \qquad \rho_3^{\langle\bar{q}q\rangle^2}(s) = \frac{1}{2}\rho_1^{\langle\bar{q}q\rangle^2}(s),$$
$$\rho_{3a}^{\langle\bar{q}q\rangle\langle\bar{q}Gq\rangle}(s) = \frac{1}{2}\rho_{1a}^{\langle\bar{q}q\rangle\langle\bar{q}Gq\rangle}(s), \qquad \rho_{3b}^{\langle\bar{q}q\rangle\langle\bar{q}Gq\rangle}(s) = -\rho_{1b}^{\langle\bar{q}q\rangle\langle\bar{q}Gq\rangle}(s). \tag{A11}$$

For the interpolating current J_2 with $J^P = 0^+$:

$$\begin{aligned}
\rho_2^{\rm pert}(s) &= \int_{\alpha_{\rm min}}^{\alpha_{\rm max}} d\alpha \int_{\beta_{\rm min}}^{\beta_{\rm max}} d\beta \frac{(1-\alpha-\beta)^2(m_1^2\beta + m_2^2\alpha - \alpha\beta s)^2}{64\pi^6} \\
&\quad \times \left[\frac{(m_1^2\beta + m_2^2\alpha - 3\alpha\beta s)(m_1^2\beta + m_2^2\alpha - \alpha\beta s)}{\alpha^3\beta^3} - \left(\frac{m_1}{\alpha} + \frac{m_2}{\beta}\right)\frac{4m_q(2m_1^2\beta + 2m_2^2\alpha - 5\alpha\beta s)}{\alpha^2\beta^2}\right], \\
\rho_2^{\langle\bar{q}q\rangle}(s) &= \langle\bar{q}q\rangle \int_{\alpha_{\rm min}}^{\alpha_{\rm max}} d\alpha \int_{\beta_{\rm min}}^{\beta_{\rm max}} d\beta \frac{(m_1^2\beta + m_2^2\alpha - \alpha\beta s)}{2\pi^4\alpha\beta} \\
&\quad \times \left[m_q(m_1^2\beta + m_2^2\alpha - 2\alpha\beta s + 8m_1m_2) - \left(\frac{m_1}{\alpha} + \frac{m_2}{\beta}\right)(1-\alpha-\beta)(2m_1^2\beta + 2m_2^2\alpha - 4\alpha\beta s)\right], \\
\rho_{2a}^{\langle GG\rangle}(s) &= \langle g_s^2 GG\rangle \int_{\alpha_{\rm min}}^{\alpha_{\rm max}} d\alpha \int_{\beta_{\rm min}}^{\beta_{\rm max}} d\beta \frac{(1-\alpha-\beta)^2(2m_1^2\beta + 2m_2^2\alpha - 3\alpha\beta s)}{384\pi^6}\left(\frac{m_1^2}{\alpha^3} + \frac{m_2^2}{\beta^3}\right), \\
\rho_{2b}^{\langle GG\rangle}(s) &= \langle g_s^2 GG\rangle \int_{\alpha_{\rm min}}^{\alpha_{\rm max}} d\alpha \int_{\beta_{\rm min}}^{\beta_{\rm max}} d\beta \frac{(1-\alpha-\beta)(m_1^2\beta + m_2^2\alpha - 2\alpha\beta s)(m_1^2\beta + m_2^2\alpha - \alpha\beta s)}{256\pi^6\alpha\beta}\left(\frac{1}{\alpha} + \frac{1}{\beta}\right), \\
\rho_{2a}^{\langle\bar{q}Gq\rangle}(s) &= \langle\bar{q}g_s\sigma\cdot Gq\rangle \int_{\alpha_{\rm min}}^{\alpha_{\rm max}} d\alpha \int_{\beta_{\rm min}}^{\beta_{\rm max}} d\beta \frac{(2m_1^2\beta + 2m_2^2\alpha - 3\alpha\beta s)}{4\pi^4}\left(\frac{m_1}{\alpha} + \frac{m_2}{\beta}\right), \\
\rho_{2b}^{\langle\bar{q}Gq\rangle}(s) &= -\frac{m_q m_1 m_2\langle\bar{q}g_s\sigma\cdot Gq\rangle}{\pi^4}\left[\left(1 + \frac{m_1^2 - m_2^2}{s}\right)^2 - \frac{4m_1^2}{s}\right]^{1/2}, \\
\rho_2^{\langle\bar{q}q\rangle^2}(s) &= \frac{2\langle\bar{q}q\rangle^2}{3\pi^2}\left[\left(1 + \frac{m_1^2 - m_2^2}{s}\right)^2 - \frac{4m_1^2}{s}\right]^{1/2}\left\{4m_1m_2 - \frac{m_q m_1(m_1^2 - m_2^2 - s) + m_q m_2(m_1^2 - m_2^2 + s)}{s}\right. \\
&\quad + \frac{m_q m_1}{s[(m_1^2 - m_2^2 - s)^2 - 4m_2^2 s]}[m_1^6 - m_2^6 + m_2^4 s - m_1^4(3m_2^2 + 2s) + m_1^2(3m_2^4 + m_2^2 s + s^2)] \\
&\quad \left. + \frac{m_q m_2}{s[(m_1^2 - m_2^2 - s)^2 - 4m_2^2 s]}[m_1^6 - m_1^4(3m_2^2 + s) + m_1^2(3m_2^4 - m_2^2 s) - (m_2^3 - m_2 s)^2]\right\}, \\
\rho_2^{\langle\bar{q}q\rangle\langle\bar{q}Gq\rangle}(s) &= \frac{4\langle\bar{q}q\rangle\langle\bar{q}Gq\rangle}{3\pi^2}\int_0^1 d\alpha \frac{m_1 m_2^3}{\alpha^2}\delta'\left[s - \frac{m_1^2\alpha + m_2^2(1-\alpha)}{\alpha(1-\alpha)}\right].
\end{aligned} \tag{A12}$$

For the interpolating current J_4 with $J^P = 0^+$:

$$\rho_4^{\rm pert}(s) = \frac{1}{2}\rho_2^{\rm pert}(s), \qquad \rho_4^{\langle\bar{q}q\rangle}(s) = \frac{1}{2}\rho_2^{\langle\bar{q}q\rangle}(s), \qquad \rho_{4a}^{\langle GG\rangle}(s) = \frac{1}{2}\rho_{2a}^{\langle GG\rangle}(s), \qquad \rho_{4b}^{\langle GG\rangle}(s) = -\rho_{2b}^{\langle GG\rangle}(s),$$
$$\rho_{4a}^{\langle\bar{q}Gq\rangle}(s) = \frac{1}{2}\rho_{2a}^{\langle\bar{q}Gq\rangle}(s), \qquad \rho_{4b}^{\langle\bar{q}Gq\rangle}(s) = \frac{1}{2}\rho_{2b}^{\langle\bar{q}Gq\rangle}(s), \qquad \rho_3^{\langle\bar{q}q\rangle^2}(s) = \frac{1}{2}\rho_1^{\langle\bar{q}q\rangle^2}(s), \qquad \rho_4^{\langle\bar{q}q\rangle\langle\bar{q}Gq\rangle}(s) = \frac{1}{2}\rho_2^{\langle\bar{q}q\rangle\langle\bar{q}Gq\rangle}(s). \tag{A13}$$

For the interpolating current J_1 with $J^P = 1^+$:

$$\begin{aligned}
\rho_1^{\mathrm{pert}}(s) &= \int_{\alpha_{\min}}^{\alpha_{\max}} d\alpha \int_{\beta_{\min}}^{\beta_{\max}} d\beta \frac{(1-\alpha-\beta)^2(m_1^2\beta+m_2^2\alpha-\alpha\beta s)^2}{512\pi^6}\left[\frac{4m_q m_2(m_1^2\beta+m_2^2\alpha-\alpha\beta s)}{\alpha^2\beta^3}\right. \\
&\quad \left. + \frac{(m_1^2\beta+m_2^2\alpha-5\alpha\beta s)(m_1^2\beta+m_2^2\alpha-\alpha\beta s)}{\alpha^3\beta^3} - \left(\frac{m_1}{\alpha}+\frac{m_2}{\beta}\right)\frac{4m_q(2m_1^2\beta+2m_2^2\alpha-5\alpha\beta s)}{\alpha^2\beta^2}\right], \\
\rho_1^{\langle\bar{q}q\rangle}(s) &= \langle\bar{q}q\rangle \int_{\alpha_{\min}}^{\alpha_{\max}} d\alpha \int_{\beta_{\min}}^{\beta_{\max}} d\beta \frac{(m_1^2\beta+m_2^2\alpha-\alpha\beta s)}{16\pi^4}\left[\frac{m_2(1-\alpha-\beta)(m_1^2\beta+m_2^2\alpha-\alpha\beta s)}{\alpha\beta^2}\right. \\
&\quad \left. + \frac{m_q(m_1^2\beta+m_2^2\alpha-3\alpha\beta s+4m_1m_2)}{\alpha\beta} - \left(\frac{m_1}{\alpha}+\frac{m_2}{\beta}\right)\frac{2(1-\alpha-\beta)(m_1^2\beta+m_2^2\alpha-2\alpha\beta s)}{\alpha\beta}\right], \\
\rho_{1a}^{\langle GG\rangle}(s) &= \langle g_s^2GG\rangle \int_{\alpha_{\min}}^{\alpha_{\max}} d\alpha \int_{\beta_{\min}}^{\beta_{\max}} d\beta \frac{(1-\alpha-\beta)^2(m_1^2\beta+m_2^2\alpha-2\alpha\beta s)}{1536\pi^6}\left(\frac{m_1^2}{\alpha^3}+\frac{m_2^2}{\beta^3}\right), \\
\rho_{1b}^{\langle GG\rangle}(s) &= \langle g_s^2GG\rangle \int_{\alpha_{\min}}^{\alpha_{\max}} d\alpha \int_{\beta_{\min}}^{\beta_{\max}} d\beta \\
&\quad \times \frac{(1-\alpha-\beta)(m_1^2\beta+m_2^2\alpha-\alpha\beta s)}{6144\pi^6\alpha\beta}\left(\frac{3m_1^2\beta+3m_2^2\alpha-5\alpha\beta s}{\alpha}-\frac{3m_1^2\beta+3m_2^2\alpha-9\alpha\beta s}{\beta}\right), \\
\rho_{1a}^{\langle\bar{q}Gq\rangle}(s) &= \langle\bar{q}g_s\sigma\cdot Gq\rangle \int_{\alpha_{\min}}^{\alpha_{\max}} d\alpha \int_{\beta_{\min}}^{\beta_{\max}} d\beta \left[\frac{m_1(2m_1^2\beta+2m_2^2\alpha-3\alpha\beta s)}{32\pi^4\alpha}+\frac{m_2(m_1^2\beta+m_2^2\alpha-2\alpha\beta s)}{32\pi^4\beta}\right], \\
\rho_{1b}^{\langle\bar{q}Gq\rangle}(s) &= \langle\bar{q}g_s\sigma\cdot Gq\rangle \int_{\alpha_{\min}}^{\alpha_{\max}} d\alpha \int_{\beta_{\min}}^{\beta_{\max}} d\beta \left[\frac{m_2(1-\alpha-\beta)(m_1^2\beta+m_2^2\alpha-2\alpha\beta s)}{64\pi^4\beta^2}-\frac{m_qm_1m_2}{64\pi^4\beta}\right], \\
\rho_{1c}^{\langle\bar{q}Gq\rangle}(s) &= -\frac{m_qm_1m_2\langle\bar{q}g_s\sigma\cdot Gq\rangle}{16\pi^4}\left[\left(1+\frac{m_1^2-m_2^2}{s}\right)^2-\frac{4m_1^2}{s}\right]^{1/2}, \\
\rho_1^{\langle\bar{q}q\rangle^2}(s) &= \frac{\langle\bar{q}q\rangle^2}{24\pi^2}\left[\left(1+\frac{m_1^2-m_2^2}{s}\right)^2-\frac{4m_1^2}{s}\right]^{1/2}\left\{4m_1m_2-\frac{2m_qm_1(m_1^2-m_2^2-s)+m_qm_2(m_1^2-m_2^2+s)}{s}\right. \\
&\quad + \frac{2m_qm_1}{s[(m_1^2-m_2^2-s)^2-4m_2^2s]}[m_1^6-m_2^6+m_2^4s-m_1^4(3m_2^2+2s)+m_1^2(3m_2^4+m_2^2s+s^2)] \\
&\quad \left. + \frac{2m_qm_2}{s[(m_1^2-m_2^2-s)^2-4m_2^2s]}[m_1^6-m_1^4(3m_2^2+s)+m_1^2(3m_2^4-m_2^2s)-(m_2^3-m_2s)^2]\right\}, \\
\rho_{1a}^{\langle\bar{q}q\rangle\langle\bar{q}Gq\rangle}(s) &= \frac{\langle\bar{q}q\rangle\langle\bar{q}Gq\rangle}{12\pi^2}\int_0^1 d\alpha \frac{m_1m_2^3}{\alpha^2}\delta'\left[s-\frac{m_1^2\alpha+m_2^2(1-\alpha)}{\alpha(1-\alpha)}\right], \\
\rho_{1b}^{\langle\bar{q}q\rangle\langle\bar{q}Gq\rangle}(s) &= \frac{\langle\bar{q}q\rangle\langle\bar{q}Gq\rangle}{48\pi^2}\int_0^1 d\alpha \frac{m_1m_2}{\alpha}\delta\left[s-\frac{m_1^2\alpha+m_2^2(1-\alpha)}{\alpha(1-\alpha)}\right].
\end{aligned} \tag{A14}$$

For the interpolating current J_3 with $J^P = 1^+$:

$$\begin{aligned}
&\rho_3^{\mathrm{pert}}(s) = \frac{1}{2}\rho_1^{\mathrm{pert}}(s), \qquad \rho_3^{\langle\bar{q}q\rangle}(s) = \frac{1}{2}\rho_1^{\langle\bar{q}q\rangle}(s), \qquad \rho_{3a}^{\langle GG\rangle}(s) = \frac{1}{2}\rho_{1a}^{\langle GG\rangle}(s), \qquad \rho_{3b}^{\langle GG\rangle}(s) = -\rho_{1b}^{\langle GG\rangle}(s), \\
&\rho_{3a}^{\langle\bar{q}Gq\rangle}(s) = \frac{1}{2}\rho_{1a}^{\langle\bar{q}Gq\rangle}(s), \qquad \rho_{3b}^{\langle\bar{q}Gq\rangle}(s) = -\rho_{1b}^{\langle\bar{q}Gq\rangle}(s), \qquad \rho_{3c}^{\langle\bar{q}Gq\rangle}(s) = \frac{1}{2}\rho_{1c}^{\langle\bar{q}Gq\rangle}(s), \qquad \rho_3^{\langle\bar{q}q\rangle^2}(s) = \frac{1}{2}\rho_1^{\langle\bar{q}q\rangle^2}(s), \\
&\rho_{3a}^{\langle\bar{q}q\rangle\langle\bar{q}Gq\rangle}(s) = \frac{1}{2}\rho_{1a}^{\langle\bar{q}q\rangle\langle\bar{q}Gq\rangle}(s), \qquad \rho_{3b}^{\langle\bar{q}q\rangle\langle\bar{q}Gq\rangle}(s) = -\rho_{1b}^{\langle\bar{q}q\rangle\langle\bar{q}Gq\rangle}(s).
\end{aligned} \tag{A15}$$

For the interpolating current J_2 with $J^P = 1^+$:

$$
\begin{aligned}
\rho_2^{\rm pert}(s) &= \int_{\alpha_{\min}}^{\alpha_{\max}} d\alpha \int_{\beta_{\min}}^{\beta_{\max}} d\beta \frac{(1-\alpha-\beta)^2(m_1^2\beta+m_2^2\alpha-\alpha\beta s)^2}{512\pi^6}\left[\frac{4m_q m_1(m_1^2\beta+m_2^2\alpha-\alpha\beta s)}{\alpha^3\beta^2}\right.\\
&\quad\left.+\frac{(m_1^2\beta+m_2^2\alpha-5\alpha\beta s)(m_1^2\beta+m_2^2\alpha-\alpha\beta s)}{\alpha^3\beta^3}-\left(\frac{m_1}{\alpha}+\frac{m_2}{\beta}\right)\frac{4m_q(2m_1^2\beta+2m_2^2\alpha-5\alpha\beta s)}{\alpha^2\beta^2}\right],\\
\rho_2^{\langle\bar{q}q\rangle}(s) &= \langle\bar{q}q\rangle \int_{\alpha_{\min}}^{\alpha_{\max}} d\alpha \int_{\beta_{\min}}^{\beta_{\max}} d\beta \frac{(m_1^2\beta+m_2^2\alpha-\alpha\beta s)}{16\pi^4}\left[\frac{m_1(1-\alpha-\beta)(m_1^2\beta+m_2^2\alpha-\alpha\beta s)}{\alpha^2\beta}\right.\\
&\quad\left.+\frac{m_q(m_1^2\beta+m_2^2\alpha-3\alpha\beta s+4m_1m_2)}{\alpha\beta}-\left(\frac{m_1}{\alpha}+\frac{m_2}{\beta}\right)\frac{2(1-\alpha-\beta)(m_1^2\beta+m_2^2\alpha-2\alpha\beta s)}{\alpha\beta}\right],\\
\rho_{2a}^{\langle GG\rangle}(s) &= \langle g_s^2GG\rangle \int_{\alpha_{\min}}^{\alpha_{\max}} d\alpha \int_{\beta_{\min}}^{\beta_{\max}} d\beta \frac{(1-\alpha-\beta)^2(m_1^2\beta+m_2^2\alpha-2\alpha\beta s)}{1536\pi^6}\left(\frac{m_1^2}{\alpha^3}+\frac{m_2^2}{\beta^3}\right),\\
\rho_{2b}^{\langle GG\rangle}(s) &= \langle g_s^2GG\rangle \int_{\alpha_{\min}}^{\alpha_{\max}} d\alpha \int_{\beta_{\min}}^{\beta_{\max}} d\beta\\
&\quad\times\frac{(1-\alpha-\beta)(m_1^2\beta+m_2^2\alpha-\alpha\beta s)}{6144\pi^6\alpha\beta}\left(\frac{3m_1^2\beta+3m_2^2\alpha-5\alpha\beta s}{\beta}-\frac{3m_1^2\beta+3m_2^2\alpha-9\alpha\beta s}{\alpha}\right),\\
\rho_{2a}^{\langle\bar{q}Gq\rangle}(s) &= \langle\bar{q}g_s\sigma\cdot Gq\rangle \int_{\alpha_{\min}}^{\alpha_{\max}} d\alpha \int_{\beta_{\min}}^{\beta_{\max}} d\beta\left[\frac{m_2(2m_1^2\beta+2m_2^2\alpha-3\alpha\beta s)}{32\pi^4\beta}+\frac{m_1(m_1^2\beta+m_2^2\alpha-2\alpha\beta s)}{32\pi^4\alpha}\right],\\
\rho_{2b}^{\langle\bar{q}Gq\rangle}(s) &= \langle\bar{q}g_s\sigma\cdot Gq\rangle \int_{\alpha_{\min}}^{\alpha_{\max}} d\alpha \int_{\beta_{\min}}^{\beta_{\max}} d\beta\left[\frac{m_1(1-\alpha-\beta)(m_1^2\beta+m_2^2\alpha-2\alpha\beta s)}{64\pi^4\alpha^2}-\frac{m_qm_1m_2}{64\pi^4\beta}\right],\\
\rho_{2c}^{\langle\bar{q}Gq\rangle}(s) &= -\frac{m_qm_1m_2\langle\bar{q}g_s\sigma\cdot Gq\rangle}{16\pi^4}\left[\left(1+\frac{m_1^2-m_2^2}{s}\right)^2-\frac{4m_1^2}{s}\right]^{1/2},\\
\rho_2^{\langle\bar{q}q\rangle^2}(s) &= \frac{\langle\bar{q}q\rangle^2}{24\pi^2}\left[\left(1+\frac{m_1^2-m_2^2}{s}\right)^2-\frac{4m_1^2}{s}\right]^{1/2}\left\{4m_1m_2-\frac{m_qm_1(m_1^2-m_2^2-s)+2m_qm_2(m_1^2-m_2^2+s)}{s}\right.\\
&\quad+\frac{2m_qm_1}{s[(m_1^2-m_2^2-s)^2-4m_2^2s]}[m_1^6-m_2^6+m_2^4s-m_1^4(3m_2^2+2s)+m_1^2(3m_2^4+m_2^2s+s^2)]\\
&\quad\left.+\frac{2m_qm_2}{s[(m_1^2-m_2^2-s)^2-4m_2^2s]}[m_1^6-m_1^4(3m_2^2+s)+m_1^2(3m_2^4-m_2^2s)-(m_2^3-m_2s)^2]\right\},\\
\rho_{2a}^{\langle\bar{q}q\rangle\langle\bar{q}Gq\rangle}(s) &= \frac{\langle\bar{q}q\rangle\langle\bar{q}Gq\rangle}{12\pi^2}\int_0^1 d\alpha\frac{m_1m_2^3}{\alpha^2}\delta'\left[s-\frac{m_1^2\alpha+m_2^2(1-\alpha)}{\alpha(1-\alpha)}\right],\\
\rho_{2b}^{\langle\bar{q}q\rangle\langle\bar{q}Gq\rangle}(s) &= \frac{\langle\bar{q}q\rangle\langle\bar{q}Gq\rangle}{48\pi^2}\int_0^1 d\alpha\frac{m_1m_2}{\alpha}\delta\left[s-\frac{m_1^2\alpha+m_2^2(1-\alpha)}{\alpha(1-\alpha)}\right].
\end{aligned}
\tag{A16}
$$

For the interpolating current J_4 with $J^P = 1^+$:

$$
\begin{aligned}
&\rho_4^{\rm pert}(s)=\frac{1}{2}\rho_2^{\rm pert}(s),\qquad \rho_4^{\langle\bar{q}q\rangle}(s)=\frac{1}{2}\rho_2^{\langle\bar{q}q\rangle}(s),\qquad \rho_{4a}^{\langle GG\rangle}(s)=\frac{1}{2}\rho_{2a}^{\langle GG\rangle}(s),\qquad \rho_{4b}^{\langle GG\rangle}(s)=-\rho_{2b}^{\langle GG\rangle}(s),\\
&\rho_{4a}^{\langle\bar{q}Gq\rangle}(s)=\frac{1}{2}\rho_{2a}^{\langle\bar{q}Gq\rangle}(s),\qquad \rho_{4b}^{\langle\bar{q}Gq\rangle}(s)=-\rho_{2b}^{\langle\bar{q}Gq\rangle}(s),\qquad \rho_{4c}^{\langle\bar{q}Gq\rangle}(s)=\frac{1}{2}\rho_{2c}^{\langle\bar{q}Gq\rangle}(s),\qquad \rho_4^{\langle\bar{q}q\rangle^2}(s)=\frac{1}{2}\rho_2^{\langle\bar{q}q\rangle^2}(s),\\
&\rho_{4a}^{\langle\bar{q}q\rangle\langle\bar{q}Gq\rangle}(s)=\frac{1}{2}\rho_{2a}^{\langle\bar{q}q\rangle\langle\bar{q}Gq\rangle}(s),\qquad \rho_{4b}^{\langle\bar{q}q\rangle\langle\bar{q}Gq\rangle}(s)=-\rho_{2b}^{\langle\bar{q}q\rangle\langle\bar{q}Gq\rangle}(s).
\end{aligned}
\tag{A17}
$$

For the mixed interpolating currents J^m and J_μ^m, we just calculate the mixed parts $\langle 0|T[J_1J_2^\dagger]|0\rangle + \langle 0|T[J_2J_1^\dagger]|0\rangle$ and $\langle 0|T[J_{1\mu}J_{2\nu}^\dagger]|0\rangle + \langle 0|T[J_{2\mu}J_{1\nu}^\dagger]|0\rangle$ in the correlation functions. The mixed part of the spectral density for J^m with $J^P = 0^+$ is

$$
\begin{aligned}
\rho_m^{\rm pert}(s) &= 0,\\
\rho_m^{\langle\bar qq\rangle}(s) &= 0,\\
\rho_m^{\langle GG\rangle}(s) &= \langle g_s^2GG\rangle\int_{\alpha_{\min}}^{\alpha_{\max}}d\alpha\int_{\beta_{\min}}^{\beta_{\max}}d\beta\frac{5m_1m_2(m_1^2\beta+m_2^2\alpha-\alpha\beta s)}{1024\pi^6\alpha\beta}\left[\frac{1-\beta}{\alpha}+\frac{1-\alpha}{\beta}-\frac{(1-\alpha-\beta)^2}{2\alpha\beta}-3\right],\\
\rho_m^{\langle\bar qGq\rangle}(s) &= \langle\bar qg_s\sigma\cdot Gq\rangle\int_{\alpha_{\min}}^{\alpha_{\max}}d\alpha\int_{\beta_{\min}}^{\beta_{\max}}d\beta\frac{5(2m_1^2\beta+2m_2^2\alpha-3\alpha\beta s)}{128\pi^4}\left[\frac{m_1(1-\beta)}{\alpha^2}+\frac{m_2(1-\alpha)}{\beta^2}-\frac{2m_1-m_q}{\alpha}-\frac{2m_2-m_q}{\beta}\right],\\
\rho_m^{\langle\bar qq\rangle^2}(s) &= 0,\\
\rho_m^{\langle\bar qq\rangle\langle\bar qGq\rangle}(s) &= \frac{5\langle\bar qq\rangle\langle\bar qGq\rangle}{48\pi^2}\int_0^1 d\alpha\left\{\frac{m_1^2\alpha+m_2^2(1-\alpha)}{2\alpha(1-\alpha)}\delta\left[s-\frac{m_1^2\alpha+m_2^2(1-\alpha)}{\alpha(1-\alpha)}\right]+H\left[s-\frac{m_1^2\alpha+m_2^2(1-\alpha)}{\alpha(1-\alpha)}\right]\right\}.
\end{aligned}
\tag{A18}
$$

For the mixed interpolating current J_μ^m with $J^P=1^+$:

$$
\begin{aligned}
\rho_m^{\rm pert}(s) &= 0,\\
\rho_m^{\langle\bar qq\rangle}(s) &= 0,\\
\rho_m^{\langle GG\rangle}(s) &= \langle g_s^2GG\rangle\int_{\alpha_{\min}}^{\alpha_{\max}}d\alpha\int_{\beta_{\min}}^{\beta_{\max}}d\beta\frac{5m_1m_2(m_1^2\beta+m_2^2\alpha-\alpha\beta s)}{36864\pi^6\alpha\beta}\\
&\quad\times\left[\frac{(1-\alpha-\beta)^2(5+\alpha+\beta)}{\alpha\beta}-\frac{3(1-\alpha-\beta)(3+\alpha+\beta)(\alpha+\beta)}{\alpha\beta}+6(1+\alpha+\beta)\right],\\
\rho_m^{\langle\bar qGq\rangle}(s) &= \langle\bar qg_s\sigma\cdot Gq\rangle\int_{\alpha_{\min}}^{\alpha_{\max}}d\alpha\int_{\beta_{\min}}^{\beta_{\max}}d\beta\\
&\quad\times\frac{5(3m_1^2\beta+3m_2^2\alpha-5\alpha\beta s)}{768\pi^4}\left[\left(\frac{m_1-m_q}{\alpha}+\frac{m_2-m_q}{\beta}\right)-\left(\frac{m_1}{\alpha^2}+\frac{m_2}{\beta^2}\right)(1-\alpha-\beta)\right],\\
\rho_m^{\langle\bar qq\rangle^2}(s) &= 0,\\
\rho_m^{\langle\bar qq\rangle\langle\bar qGq\rangle}(s) &= -\frac{5\langle\bar qq\rangle\langle\bar qGq\rangle}{576\pi^2}\int_0^1 d\alpha\left\{\frac{2[m_1^2\alpha+m_2^2(1-\alpha)]}{\alpha(1-\alpha)}\delta\left[s-\frac{m_1^2\alpha+m_2^2(1-\alpha)}{\alpha(1-\alpha)}\right]\right.\\
&\quad\left.+3*H\left[s-\frac{m_1^2\alpha+m_2^2(1-\alpha)}{\alpha(1-\alpha)}\right]\right\}.
\end{aligned}
\tag{A19}
$$

[1] E. Klempt and A. Zaitsev, Phys. Rep. **454**, 1 (2007).
[2] J. Beringer *et al.* (Particle Data Group), Phys. Rev. D **86**, 010001 (2012).
[3] R. L. Jaffe, Phys. Rev. D **15**, 267 (1977).
[4] R. L. Jaffe, Phys. Rev. D **15**, 281 (1977).
[5] H.-X. Chen, A. Hosaka, and S.-L. Zhu, Phys. Rev. D **76**, 094025 (2007).
[6] H.-X. Chen, A. Hosaka, and S.-L. Zhu, Phys. Lett. B **650**, 369 (2007).
[7] A. Zhang, T. Huang, and T. G. Steele, Phys. Rev. D **76**, 036004 (2007).
[8] D. Ebert, R. N. Faustov, and V. O. Galkin, Phys. Lett. B **634**, 214 (2006).
[9] D. Ebert, R. N. Faustov, and V. O. Galkin, Eur. Phys. J. C **58**, 399 (2008).
[10] R. D. Matheus, S. Narison, M. Nielsen, and J. M. Richard, Phys. Rev. D **75**, 014005 (2007).
[11] M. E. Bracco, S. H. Lee, M. Nielsen, and R. Rodrigues da Silva, Phys. Lett. B **671**, 240 (2009).
[12] W. Chen and S.-L. Zhu, Phys. Rev. D **81**, 105018 (2010).
[13] W. Chen and S.-L. Zhu, Phys. Rev. D **83**, 034010 (2011).
[14] M.-L. Du, W. Chen, X.-L. Chen, and S.-L. Zhu, Chin. Phys. C **37**, 033104 (2013).
[15] L. Maiani, V. Riquer, F. Piccinini, and A. D. Polosa, Phys. Rev. D **72**, 031502 (2005).
[16] L. Maiani, A. D. Polosa, and V. Riquer, Phys. Rev. Lett. **99**, 182003 (2007).
[17] L. Maiani, A. D. Polosa, and V. Riquer, New J. Phys. **10**, 073004 (2008).

[18] R. T. Kleiv, T. G. Steele, A. Zhang, and I. Blokland, Phys. Rev. D **87**, 125018 (2013).

[19] J. Carlson, L. Heller, and J. A. Tjon, Phys. Rev. D **37**, 744 (1988).

[20] M. Zhang, H. Zhang, and Z. Zhang, Commun. Theor. Phys. **50**, 437 (2008).

[21] S. Pepin, F. Stancu, M. Genovese, and J. Richard, Phys. Lett. B **393**, 119 (1997).

[22] J. Vijande, A. Valcarce, and K. Tsushima, Phys. Rev. D **74**, 054018 (2006).

[23] J. Vijande, A. Valcarce, and N. Barnea, Phys. Rev. D **79**, 074010 (2009).

[24] D. M. Brink and Fl. Stancu, Phys. Rev. D **57**, 6778 (1998).

[25] B. Silvestre-Brac and C. Semay, Z. Phys. C **59**, 457 (1993).

[26] S. Zouzou, B. Silvestre-Brac, C. Gignoux, and J. Richard, Z. Phys. C **30**, 457 (1986).

[27] D. Ebert, R. N. Faustov, V. O. Galkin, and W. Lucha, Phys. Rev. D **76**, 114015 (2007).

[28] A. V. Manohar and M. B. Wise, Nucl. Phys. **B399**, 17 (1993).

[29] Y. Cui, X.-L. Chen, W.-Z. Deng, and S.-L. Zhu, High Energy Phys. Nucl. Phys. **31**, 7 (2007).

[30] M.-L. Du, W. Chen, X.-L. Chen, and S.-L. Zhu, Phys. Rev. D **87**, 014003 (2013).

[31] F. S. Navarra, M. Nielsen, and S. H. Lee, Phys. Lett. B **649**, 166 (2007).

[32] Z.-G. Wang, Y.-M. Xu, and H.-J. Wang, Commun. Theor. Phys. **55**, 1049 (2011).

[33] H. Lipkin, Phys. Lett. **45B**, 267 (1973).

[34] J. P. Ader, J. M. Richard, and P. Taxil, Phys. Rev. D **25**, 2370 (1982).

[35] H. J. Lipkin, Phys. Lett. B **172**, 242 (1986).

[36] J. M. Richard, Nucl. Phys. B, Proc. Suppl. **21**, 254 (1991).

[37] M. Bander and A. Subbaraman, Phys. Rev. D **50**, R5478 (1994).

[38] M. A. Moinester, Z. Phys. A **355**, 349 (1996).

[39] B. A. Gelman and S. Nussinov, Phys. Lett. B **551**, 296 (2003).

[40] T. Carames, A. Valcarce, and J. Vijande, Phys. Lett. B **699**, 291 (2011).

[41] G. Q. Feng, X. H. Guo, and B. S. Zou, arXiv:1309.7813.

[42] J.-R. Zhang and M.-Q. Huang, Phys. Rev. D **80**, 056004 (2009).

[43] Z.-F. Sun, X. Liu, M. Nielsen, and S.-L. Zhu, Phys. Rev. D **85**, 094008 (2012).

[44] R. M. Albuquerque, X. Liu, and M. Nielsen, Phys. Lett. B **718**, 492 (2012).

[45] M. A. Shifman, A. I. Vainshtein, and V. I. Zakharov, Nucl. Phys. **B147**, 385 (1979).

[46] L. J. Reinders, H. Rubinstein, and S. Yazaki, Phys. Rep. **127**, 1 (1985).

[47] P. Colangelo and A. Khodjamirian, Frontier Part. Phys. **3**, 1495
(2000).

[48] W. Chen, T. G. Steele, M.-L. Du, and S.-L. Zhu, Eur. Phys. J. C **74**, 2773 (2014).

[49] E. Braaten, S. Narison, and A. Pich, Nucl. Phys. **B373**, 581 (1992).

[50] S. Narison, Phys. Lett. B **707**, 259 (2012).

[51] S. Narison, Phys. Lett. B **693**, 559 (2010).

[52] J. H. Kuhn, M. Steinhauser, and C. Sturm, Nucl. Phys. **B778**, 192 (2007).

[53] W. Chen, T. G. Steele, and S.-L. Zhu, J. Phys. G **41**, 025003 (2014).